Archives of Toxicology (2020) 94:609–629
https://doi.org/10.1007/s00204-019-02638-9

ORGAN TOXICITY AND MECHANISMS

Emerging club drugs: 5-(2-aminopropyl)benzofuran (5-APB) is more toxic than its isomer 6-(2-aminopropyl)benzofuran (6-APB) in hepatocyte cellular models

Rita Roque Bravo[1] · Helena Carmo[1] · João Pedro Silva[1] · Maria João Valente[2] · Félix Carvalho[1] · Maria de Lourdes Bastos[1] · Diana Dias da Silva[1]

Received: 16 October 2019 / Accepted: 26 November 2019 / Published online: 14 December 2019

Abstract

New phenylethylamine derivatives are among the most commonly abused new psychoactive substances. They are synthesized and marketed in lieu of classical amphetaminic stimulants, with no previous safety testing. Our study aimed to determine the in vitro hepatotoxicity of two benzofurans [6-(2-aminopropyl)benzofuran (6-APB) and 5-(2-aminopropyl)benzofuran (5-APB)] that have been misused as 'legal highs'. Cellular viability was assessed through the 3-(4,5-dimethylthiazol-2-yl)-2,5-diphenyltetrazolium bromide (MTT) reduction assay, following 24-h drug exposure of human hepatoma HepaRG cells (EC_{50} 2.62 mM 5-APB; 6.02 mM 6-APB), HepG2 cells (EC_{50} 3.79 mM 5-APB; 8.18 mM 6-APB) and primary rat hepatocytes (EC_{50} 964 µM 5-APB; 1.94 mM 6-APB). Co-incubation of primary hepatocytes, the most sensitive in vitro model, with CYP450 inhibitors revealed a role of metabolism, in particular by CYP3A4, in the toxic effects of both benzofurans. Also, 6-APB and 5-APB concentration-dependently enhanced oxidative stress (significantly increased reactive species and oxidized glutathione, and decreased reduced glutathione levels) and unsettled mitochondrial homeostasis, with disruption of mitochondrial membrane potential and decline of intracellular ATP. Evaluation of cell death mechanisms showed increased caspase-8, -9, and -3 activation, and nuclear morphological changes consistent with apoptosis; at concentrations higher than 2 mM, however, necrosis prevailed. Concentration-dependent formation of acidic vesicular organelles typical of autophagy was also observed for both drugs. Overall, 5-APB displayed higher hepatotoxicity than its 6-isomer. Our findings provide new insights into the potential hepatotoxicity of these so-called 'safe drugs' and highlight the putative risks associated with their use as psychostimulants.

Key points

- The isomer 5-APB is more hepatotoxic than 6-APB.
- At biologically relevant concentrations, CYP2D6 and 3A4 contribute to the toxification of psychoactive 5-APB and 6-APB. CYP2E1 seems also implicated in 5-APB bioactivation.
- Both benzofury concentration-dependently increase oxidative species, disturb mitochondrial potential homeostasis and energetic levels.
- 5-APB and 6-APB stimulate autophagy and apoptosis at low in vitro concentrations.

Keywords *Benzofury* · Liver · Toxicity · In vitro · Bioactivation · Cell death

✉ Rita Roque Bravo
rita.rdsb@gmail.com

✉ Diana Dias da Silva
up538058@g.uporto.pt

[1] UCIBIO, REQUIMTE, Laboratory of Toxicology, Faculty of Pharmacy, University of Porto, Rua Jorge Viterbo Ferreira, 228, 4050-313 Porto, Portugal

[2] UCIBIO, REQUIMTE, Laboratory of Biochemistry, Faculty of Pharmacy, University of Porto, Rua Jorge Viterbo Ferreira, 228, 4050-313 Porto, Portugal

Introduction

The recent years have brought on an increase in the number and use of new psychoactive substances (NPS). The number of NPS that reach the online markets every year is ever growing, with over 670 new drugs being currently monitored by the European Monitoring Centre for Drugs and Drug Addiction (EMCDDA 2018). Synthetic phenylethylamines are one of the most prevalent NPS groups, as detailed by the

2018 World Drug Report (UNODC 2018), and within this group, psychoactive benzofurans or *benzofury* are among the most used drugs (Roque Bravo et al. 2019). 5-(2-Aminopropyl)benzofuran (5-APB) and 6-(2-aminopropyl)benzofuran (6-APB) have structural (Fig. 1) and pharmacological similarities to the well-known classic stimulants 3,4-methylenedioxyamphetamine (MDA) and 3,4-methylenedioxymethamphetamine (MDMA; *ecstasy*), acting as monoamine transporter inhibitors and as serotoninergic receptor agonists (Iversen et al. 2013; Rickli et al. 2015).

A few clinical reports have disclosed benzofuran toxicity (Adamowicz et al. 2014; Chan et al. 2013; Helander et al. 2015; Hofer et al. 2017; Krpo et al. 2018; McIntyre et al. 2015; Seetohul and Pounder 2013; Turcant et al. 2017; Vallersnes et al. 2017), as well as lethality (Connelly et al. 2002). Some of the deleterious effects reported by users include agitation, mydriasis, tachycardia, seizures and hallucinations, similar to symptoms reported for MDA or MDMA (Jebadurai et al. 2013).

The liver is the organ where the majority of bioactivation and detoxifying metabolic reactions take place and, considering that oral ingestion is the most common route of administration for benzofurans (Barcelo et al. 2017), it becomes clear that there is a significant first-passage effect. As such, the liver is fully engaged in the biotransformation/elimination of these substances and of the resulting metabolites. Previous works have demonstrated that amphetamines and their metabolites can induce deleterious effects on liver cells by disturbing intracellular mechanisms, such as oxidative and mitochondrial homeostasis, and by activating programmed cell death pathways (Carvalho et al. 1996, 1997, 2001, 2013a; Dias da Silva et al. 2014a, b; Pontes et al. 2008a, b). Given the structural similarity, it becomes apparent that benzofurans may also have the potential to induce such effects on hepatocytes. One recent work proved that both 5-APB and its methylated analogue, 1-(benzofuran-5-yl)-N-methylpropan-2-amine (5-MAPB) have cytotoxic effects on freshly isolated rat hepatocytes through the production of reactive species and interference with mitochondrial membrane potential (Nakagawa et al. 2017). Notwithstanding, there is still a lack of research into the potential hepatotoxic effects of other benzofurans, in particular 6-APB. Noteworthy, despite being banned on countries such as the UK (ACDM 2013), 6-APB still remains one of the top selling NPS in Europe, being the most consumed *benzofury* (Roque Bravo et al. 2019).

Herein, we provide a comparison between the hepatotoxicity of 5-APB and its popular isomer 6-APB, which is particularly relevant in the clinical and forensic contexts, as it allows first-responders, clinicians and forensic experts, to better estimate the perils of the drug they are facing against, and determine the best treatment approach.

Materials and methods

Chemicals

Both 5-APB and 6-APB were acquired online at sensearomatics.net on March 2013. Chemical purity and identity of the drugs were verified by mass spectrometry, NMR and elemental analysis. Analytical data were consistent with the assigned structures with about 99% purity. Stock solutions of both drugs were made up in Hanks' balanced salt solution (HBSS, no calcium or magnesium) and stored at – 20 °C. These solutions were thawed and diluted on the days that experiments were performed.

The cell culture reagents were purchased from Gibco (Thermo Fisher Scientific, Massachusetts, USA) and all other reagents were obtained from Sigma-Aldrich (Missouri, USA), unless otherwise stated.

Animals

Male Wistar Han rats with a body weight of 150–250 g were kept in sterile facilities under controlled temperature

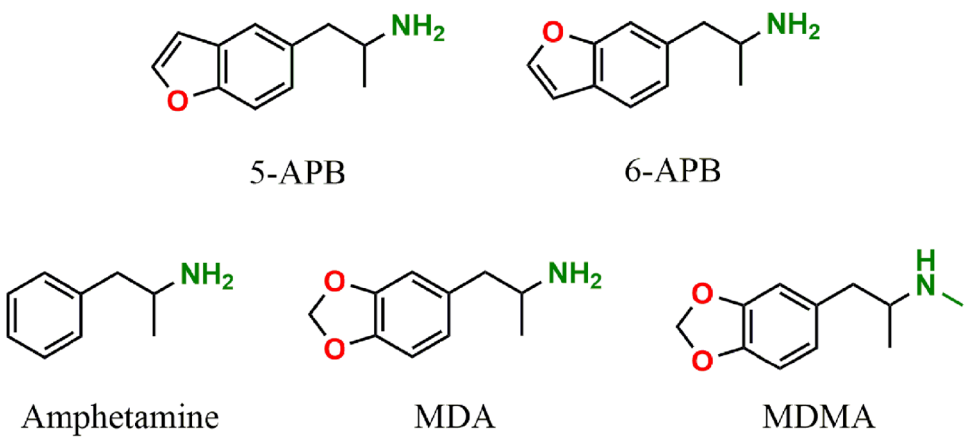

Fig. 1 Chemical structures of psychoactive benzofurans and classical amphetamines. 5-APB, 5-(2-aminopropyl)benzofuran; 6-APB, 6-(2-aminopropyl) benzofuran; MDA, 3,4-methylenedioxyamphetamine; MDMA, 3,4-methylenedioxymethamphetamine

(20 ± 2 °C), humidity (40–60%), and lighting (12-h light/dark cycle) conditions and fed with sterile standard rat chow and tap water ad libitum. Isolation of hepatocytes was always conducted between 8:00 and 10:00 a.m. Surgical procedures were performed after rat anaesthesia induced by an i.p. injection of a combination of 20 mg/kg xylazine (Rompun® 2%, Bayer HealthCare, Germany) and 100 mg/kg ketamine (Clorketam® 1000, Vétoquinol, France), and maintained through inhalation of isoflurane vapour (IsoVet® 1000 mg/g, B. Braun VetCare, Germany). This study was performed at the highest standards of ethics after approval by the local Ethical Committee for the Welfare of Experimental Animals (University of Porto-ORBEA; project 158/2014) and by the national authority *Direção Geral de Alimentação e Veterinária* (DGAV). Housing and all experimental procedures were performed by investigators accredited for laboratory animal use in accordance with the Portuguese and European legislation (law DL 113/2013, Guide for Animal Care; Directives 86/609/EEC and 2010/63/UE).

Isolation of primary rat hepatocytes

Isolation of hepatocytes was performed using a modified two-step perfusion of the liver, as previously described by Dias da Silva et al. (2017) with some modifications. The liver was perfused in situ via the vena portae, with sterile EGTA-buffer at 37 °C, for approximately 10–15 min. The chelator promoted the irreversible cleavage of the desmosomes (junctional complexes) through calcium sequestration. The EGTA-buffer consisted of 248 mL glucose solution (9 g/L D-glucose), 40 mL Krebs–Henseleit buffer (60 g/L NaCl, 1.75 g/L KCl, and 1.6 g/L KH_2PO_4; adjusted to pH 7.4), 40 mL HEPES-buffer I (60 g/L HEPES; adjusted to pH 8.5), 30 mL MEM non-essential amino acid solution (100×), 30 mL MEM amino acids solution (10×), 4 mL glutamine solution (7 g/L L-glutamine), and 1.6 mL EGTA-solution (47.5 g/L EGTA; dissolved by addition of NaOH, adjusted to pH 7.6). Subsequently, hepatic collagen was hydrolysed by liver perfusion for 10–15 min with a sterile collagenase buffer supplemented with its cofactor calcium, at 37 °C. The collagenase buffer consisted of 155 mL glucose solution, 25 mL Krebs–Henseleit buffer, 25 mL HEPES-buffer I, 15 mL MEM non-essential amino acid solution (100×), 15 mL MEM amino acids solution (10×), 10 mL $CaCl_2$ solution (19 g/L $CaCl_2{\cdot}2H_2O$), 2.5 mL glutamine solution, and ~ 300 U/mL collagenase type IA from *Clostridium histolyticum* (dissolved immediately before use). After perfusion, the liver was dissected, removed from the animal, and the hepatic capsule gently disrupted in a sterile suspension buffer [124 mL glucose solution, 20 mL KH-buffer, 20 mL HEPES-buffer II (60 g/L HEPES; adjusted to pH 7.6), 15 mL MEM non-essential amino acid solution (100×), 15 mL MEM amino acids solution (10×), 2 mL glutamine solution, 1.6 mL $CaCl_2$ solution, 0.8 mL $MgSO_4$ solution (24.6 g/L $MgSO_4{\cdot}7H_2O$), and 400 mg bovine serum albumin (BSA)]. The obtained suspension was purified by three low-speed centrifugations at 50*g*, for 2 min, at 4 °C. The viability of isolated hepatocytes at this stage was always above 90%, as assessed by the trypan blue exclusion method.

Culture of primary rat hepatocytes

A suspension of 5×10^5 viable cells/mL in complete culture medium was seeded onto the central 60 wells of 96-well plates (5×10^4 cells per well) or onto 6-well plates (1×10^6 cells per well) pre-coated with collagen. Complete cell culture medium consisted of William's E medium (Sigma-Aldrich, Missouri, USA) supplemented with 10% heat-inactivated foetal bovine serum (FBS), 5 µg/mL insulin solution from bovine pancreas (Sigma-Aldrich, Missouri, USA), 50 nM dexamethasone (Sigma-Aldrich, Missouri, USA), 1% antibiotic solution (10,000 U/mL penicillin; 10,000 µg/mL streptomycin), 100 µg/mL gentamicin, and 250 ng/mL amphotericin B. After seeding, primary rat hepatocytes were left to adhere overnight at 37 °C, in an atmosphere of 5% CO_2. On the next day, cells were exposed to the test drugs.

Human HepaRG cells

HepaRG hepatocyte cell line derives from a female patient with hepatocarcinoma. Upon reaching confluence, cells can transdifferentiate into two types of cells, one that is morphologically similar to human primary hepatocytes, and another that resembles bile canaliculus-like structures (Guillouzo et al. 2007). HepaRG cells retain the ability of expressing all major cytochrome P450 isoforms (with exception of CYP2E1 and CYP2D6) and many phase II enzymes, closely mimicking the in vivo situation (Guillouzo et al. 2007).

HepaRG cells were acquired from Life Technologies (Invitrogen, France) and were cultured as described before (Dias da Silva et al. 2017), at 37 °C, with an atmosphere of 5% CO_2, in 75-cm^2 flasks, using Williams' E medium with L-glutamine, supplemented with 10% FBS, 1% antibiotic solution (10,000 U/mL penicillin; 10,000 µg/mL streptomycin), 5 µg/mL insulin (Sigma-Aldrich, Missouri, USA), and 50 µM hydrocortisone 21-hemisuccinate sodium salt (Sigma-Aldrich, Missouri, USA). The medium was changed every 2–3 days, and cells were sub-cultured by tripsinization at around 80% confluence, for a maximum of 10 passages. Upon reaching confluence, the differentiation was initiated by replacing the medium by fresh culture medium supplemented with 2% DMSO (Merck Millipore, Massachusetts, USA). The medium was then changed every 2–3 days, for 2 weeks, to promote differentiation into a 1:1 ratio of hepatic cells:biliary cells, as confirmed by microscopic observation. At the end of the differentiation period, cells were seeded

onto 96-well plates at a density of 1.44×10^5 cells per well in a volume of 200 µL of complete medium and left to adhere overnight. They were used for cytotoxicity assays on the following day.

Human HepG2 cells

HepG2 cells, which derive from a male patient with hepatoblastoma, also express normal hepatocyte function. These cells secrete the majority of plasma proteins into the culture medium and retain the ability to produce and secrete bile acids (Bouma et al. 1989). These cells were previously used to successfully demonstrate the hepatotoxicity of other stimulants, namely amphetamines (Dias da Silva et al. 2013a, 2014a, b; Bouma et al. 1989) and piperazines (Dias da Silva et al. 2013b).

HepG2 cells were acquired from Life Technologies (Invitrogen, France) and cultured as previously described, with some modifications (Dias da Silva et al. 2013b). Briefly, the cells were kept in DMEM medium supplemented with 10% FBS and 1% antibiotic solution (10,000 U/mL penicillin; 10,000 µg/mL streptomycin), in 75-cm^2 flasks, under a humidified 5% CO_2 atmosphere at 37 °C, and subjected to regular medium changes (every 2–3 days). Whenever cells reached 80% confluence, they were sub-cultured by tripsinization for no more than 10 passages. For the cytotoxicity assays, cells were seeded in 96-well plates, at a density of 80×10^4 cells per well, in a volume of 200 µL of complete medium, and left to adhere overnight.

Drug exposures

On the day of the experiments, primary hepatocytes, HepaRG cells, and HepG2 cells were exposed to the test drugs for 24 h. The concentration range tested for each drug in the 3-(4,5-dimethylthiazol-2-yl)-2,5-diphenyltetrazolium bromide (MTT) reduction assay across the three different cell models is displayed in Table 1. MTT data were then used to calculate the concentrations of each drug to be tested in the following assays, which were conducted in rat primary hepatocytes only, due to the increased sensibility displayed by these cells. Accordingly, the concentrations of each drug producing 20%, 40%, 50% and 70% of the maximum cytotoxic effect in the MTT assay, i.e. EC_{20}, EC_{40}, EC_{50} and EC_{70}, respectively, were estimated from the respective concentration versus response curves, using the parameters of the best fit regression model (see "Results" section). The selected concentrations are in line with those previously tested for amphetamine derivatives (Dias da Silva et al. 2014a).

Table 1 Concentrations (µM) of 5-(aminopropyl)benzofuran (5-APB) and 6-(aminopropyl)benzofuran (6-APB) tested for evaluating drug-induced alterations on cell viability, as assessed by the 3-(4,5-dimethylthiazol-2-yl)-2,5-diphenyltetrazolium bromide (MTT) reduction assay, after 24 h at 37 °C

	5-APB (µM)	6-APB (µM)
Primary rat hepatocytes	3.77×10^1–1.00×10^4	3.77×10^1–2.30×10^4
HepaRG cells	1.10×10^2–6.50×10^3	1.17×10^3–1.40×10^4
HepG2 cells	2.93×10^2–2.00×10^4	1.92×10^2–3.00×10^4

Cellular viability by the MTT reduction assay

The cytotoxicity of the drugs was evaluated using the MTT reduction assay, as described previously (Dias da Silva et al. 2015). The assay assesses cell viability through the indirect measurement of the activity of reductases that convert yellow soluble MTT into purple insoluble formazan salts. As MTT can only be reduced when these enzymes are active, the reaction is used as an indicator of the cell metabolic competence and, therefore, of viability. Briefly, after the exposure period, the culture medium was aspirated, followed by the addition of fresh culture medium containing 0.25 mg/L MTT in HBSS (no calcium, no magnesium). After a 30-min incubation at 37 °C in a humidified, 5% CO_2 atmosphere, the formed intracellular crystals of formazan were dissolved in 100 µL DMSO. The absorbance was measured at 570 nm, using a multi-well plate reader (BioTek Instruments, Vermont, USA). Data were normalized to positive (1% Triton X-100) and negative controls (culture medium only).

Cytochrome P450 inhibition

To determine the influence of CYP metabolism in the toxicity induced by these drugs, different CYP isoforms of primary rat hepatocytes were inhibited prior and during exposure to the test drugs, as described before (Dias da Silva et al. 2013b). Briefly, the cells were incubated for 1 h with four CYP inhibitors: 500 µM metyrapone (CYP2E1 inhibitor), 10 µM quinidine (CYP2D6 inhibitor), 1 µM ketoconazole (CYP3A4 inhibitor) and 1 mM 1-aminobenzotriazole (ABT; general CYP inhibitor). Then, cells were co-incubated with these inhibitors and each test drug, during 24 h, at 37 °C. Afterwards, cell viability was evaluated using the MTT assay and data were normalized to positive (1% Triton X-100) and negative (cell culture medium only) controls. Additional controls with inhibitor only in cell culture medium were performed and compared to negative controls to ensure that no cytotoxicity derived from these treatments.

Intracellular reactive oxygen (ROS) and nitrogen (RNS) species

The assessment of intracellular reactive oxygen (ROS) and nitrogen (RNS) species was performed using the 2′,7′-dichlorodihydrofluorescein diacetate (DCFH-DA) fluorescence assay, as described by Dias da Silva et al. (2014a). Briefly, primary rat hepatocytes seeded onto 96-well plates were exposed for 30 min to 10 µM DCFH-DA, at 37 °C, protected from light. Afterwards, the cells were washed with HBSS (no calcium, no magnesium) and incubated with each tested drug, at 37 °C, for 24 h. The fluorescence was recorded using a fluorescence microplate reader (BioTek Instruments, Vermont, USA), set to 485 nm excitation and 530 nm emission. The acquired data were normalized to control conditions (only cell culture medium).

Total (tGSH), reduced (GSH), and oxidized (GSSG) glutathione

Primary rat hepatocytes seeded onto 6-well plates were exposed to each drug for 24 h, at 37 °C. After this time, cells were washed with HBSS (no calcium, no magnesium) and precipitated with 10% perchloric acid for 20 min, at 4 °C. Cells were then scrapped and the obtained suspension was centrifuged at 13,000*g* for 5 min, at 4 °C. The supernatant was collected and stored at − 80 °C until further determinations. The cell pellet was resuspended in 1 M NaOH and used to quantify protein by the Lowry assay (Lowry et al. 1951). After thawing, the supernatants were neutralized using 0.76 M $KHCO_3$ (1:1) and centrifuged at 13,000*g* for 10 min, at 4 °C. Supernatants were then used to determine total glutathione (tGSH), oxidized glutathione (GSSG) and ATP.

The 5,5-dithio-bis(2-nitrobenzoic acid) (DTNB)-GSSG reductase-recycling assay was used to measure tGSH, as previously described (Dias da Silva et al. 2014a). Briefly, 100 µL of each neutralised sample, blank and standard were transferred into a 96-well plate, followed by the addition of 65 µL reagent solution (72 mM phosphate buffer, 0.69 mM NADPH, and 4 mM DTNB). The plates were incubated for 15 min, at 30 °C, in a multi-well plate reader (Power Wave X™, BioTek Instruments, Inc.) and then 40 µL of a 10 U/mL glutathione reductase solution was added. The absorbance was further read in kinetic mode at 415 nm to follow the formation of 5-thio-2-nitrobenzoic acid (TNB). The GSH content in the samples was interpolated from a standard curve, performed for every independent experiment. As 2-vinylpyridine blocks GSH, the same protocol was used for the quantification of GSSG, following sample incubation with 2-vinylpyridine for 1 h, at 4 °C. Experimental data were normalized to the protein content of each sample and the intracellular reduced glutathione (GSH) was calculated using the formula $GSH = tGSH - 2 \times GSSG$.

Intracellular adenosine triphosphate (ATP)

A bioluminescence method was used for measuring intracellular ATP, as previously described Dias da Silva et al. (2013b). Samples were prepared as detailed above for the determination of glutathione. Afterwards, 75 µL of each sample neutralized supernatant, standard, or blank were transferred into a white 96-well plate. Then, 75 µL of a luciferin–luciferase solution (0.15 mM luciferin; 30,000 light units luciferase/mL; 10 mM $MgSO_4$; 50 mM glycine; 1 mM Tris; 0.55 mM EDTA; 1% BSA) were added and the emitting light intensity was measured using a luminescence plate reader (BioTek Instruments, Vermont, USA). The ATP content in the samples was interpolated from a standard curve performed in every experiment and normalized to the protein content.

Mitochondrial membrane potential (Δψm)

Mitochondrial integrity was evaluated using tetramethylrhodamine ethyl ester (TMRE), a positive-charged dye that solely targets active mitochondria. As described by Dias da Silva et al. (2013b), primary rat hepatocytes seeded onto 96-well plates were exposed to the drugs for 24 h at 37 °C. Following drug exposure, the medium was aspirated, and cells were washed with HBSS (no calcium, no magnesium) and incubated for 30 min with 2 µM TMRE prepared in fresh culture medium, protected from light. After the incubation period, cells were washed twice with HBSS (no calcium and no magnesium) and the fluorescence was quantified using a fluorescence microplate reader, set to 544 nm excitation and 590 nm emission. Data were normalized to negative controls (cell culture medium only).

Caspase-8, -9, and -3 activities

The activity of pro-apoptotic caspases-8, -9, and -3 was evaluated in primary rat hepatocytes seeded onto 6-well plates, following 24-h drug exposures at 37 °C. The incubation medium was discarded, the cells washed with HBSS (no calcium, no magnesium) and added of 150 µL lysis buffer (50 mM HEPES, 0.1 mM EDTA, 0.1% CHAPS, and 1 mM DTT; pH 7.4). The plates were then placed at 4 °C for 30 min, and cells scraped, collected into 2 mL microcentrifuge tubes, and centrifuged at 13,000*g* for 10 min, at 4 °C. Then, 50 µL of the supernatant were collected into a 96-well plate and added of 200 µL assay buffer (100 mM NaCl, 50 mM HEPES, 0.1 mM EDTA, 10% glycerol, 0.1% CHAPS, and 1 mM DTT). The reaction was started by adding 5 µL of caspase-3 (Ac-DEVD-pNA; 4 mM in DMSO),

caspase-8 (Ac-IETD-pNA; 10 mM in DMSO), or caspase-9 (Ac-LEHD-pNA; 10 mM in DMSO) substrates. The plates were then sealed with parafilm, covered with aluminium foil, and incubated at 37 °C for 24 h. After this period, the absorbance was measured at 405 nm and data were normalized to the amount of protein of each sample. The protein content in the cytoplasmic fraction was quantified using the DC™ protein assay kit (Bio-Rad Laboratories, CA, USA), as described by the manufacturer. Results were expressed as percentage of negative controls.

Extracellular lactate dehydrogenase (LDH)

Cell lactate dehydrogenase (LDH) leakage occurs upon rupture of the cytoplasmic membrane. After a 24-h exposure to each drug, 10 µL of the incubation medium of primary rat hepatocytes seeded in 96-well plates were added of 40 µL of 50 mM potassium phosphate buffer and 200 µL of 0.2 mM β-NADH (in 50 mM potassium phosphate buffer), as described by Dias da Silva (2019). Then, the addition of 25 µL of 22.72 mM sodium pyruvate (in 50 mM potassium phosphate buffer) initiated the oxidation of β-NADH into β-NAD^+, which was monitored by reading the absorbance decay at 340 nm, every 16 s, for 3 min, using an automatic plate reader Power Wave X™ (BioTek Instruments, Inc.). Data were normalized to positive (1% Triton X-100) and negative (cell culture medium only) controls.

Hoechst 33342/propidium iodide (PI) fluorescent staining

Hoechst 33342 is a cell-permanent counterstain that binds to DNA and emits a blue fluorescence; and propidium iodide (PI) is a nuclear membrane impermeant dye that issues red fluorescence solely in dead cells. In order to identify hepatocytes undergoing apoptosis or necrosis, Hoechst 33342 and PI were used as staining probes, as previously described by Valente et al. (2016). Briefly, after washing hepatocytes seeded onto 6-well plates with HBSS (no calcium, no magnesium), cells were incubated with 50 µM PI for 15 min, under light protection, rinsed twice, and further incubated with 5 µg/mL Hoechst 33342 for 5 min, previous to observation under an inverted fluorescence microscope Nikon Eclipse Ti (Nikon, Amsterdam, Netherlands), at an original magnification of 200×.

Acridine orange staining for acidic vesicular organelles (AVO)

Acidic vesicular organelles (AVO) formation was assessed through acridine orange staining, as described in Valente et al. (2017). This lysosomotropic dye issues green/yellow/orange/red fluorescence in a pH-dependent manner: at neutral pH it is a hydrophobic green molecule; inside acidic organelles it is converted into its protonated form, building aggregates that issue yellow-to-red fluorescence. Briefly, following exposure, hepatocytes were incubated with 5 µg/mL acridine orange for 20 min, at 37 °C, to detect AVOs formation. Following incubation with acridine orange, cells were rinsed three times with HBSS (no calcium, no magnesium) and observed under an inverted fluorescence microscope Nikon Eclipse Ti (Nikon, Amsterdam, Netherlands), at an original magnification of 200×.

Statistical analysis

Data obtained in the MTT assay in four independent experiments were fitted to the Logit model, chosen based on a goodness-to-fit principle (best fit dosimetric model) (Dias da Silva et al. 2013c). Comparisons between concentration–response curves were performed using the extra sum-of-squares *F* test. All other assays were performed at least in three independent experiments and data are presented as mean ± standard error of the mean (SEM). The normality of data distribution was analysed using the Kolmogorov–Smirnov test, and statistical comparisons between groups were done using one-way analysis of variance (ANOVA), followed by Dunn's multiple comparison test, when the results followed a Gaussian distribution; or otherwise by Kruskal–Wallis test. All statistical analyses were made using GraphPad Prism® software, version 6.07 (San Diego, CA, USA).

Results

5-APB was more hepatotoxic than 6-APB in all of the tested hepatocyte models

The in vitro cytotoxic effects observed for the tested drugs in the different hepatocyte models are presented in Fig. 2. Our data show that the drug-induced decrease in cell viability is concentration-dependent for both drugs in all tested cell models. As observed by the respective potencies of each drug (Fig. 2, Table 2), 5-APB elicited greater cytotoxicity than 6-APB, in all the tested in vitro models ($p < 0.0001$; *F* test). It is also clear that primary rat hepatocytes display higher sensitivity to the hepatotoxicity elicited by 5-APB and 6-APB, than human immortalized hepatocytes ($p < 0.0001$; *F* test). In addition, HepG2 cells revealed to be more resistant to the toxic effects of these drugs than HepaRG cells ($p < 0.0001$; *F* test). Accordingly, the curves obtained for HepG2 cells were shifted to the right and the EC_{50} values were higher, when compared to those obtained for HepaRG cells (Fig. 2, Table 2). Based on the relative sensitivities of these in vitro models to benzofuran toxicity, further assays

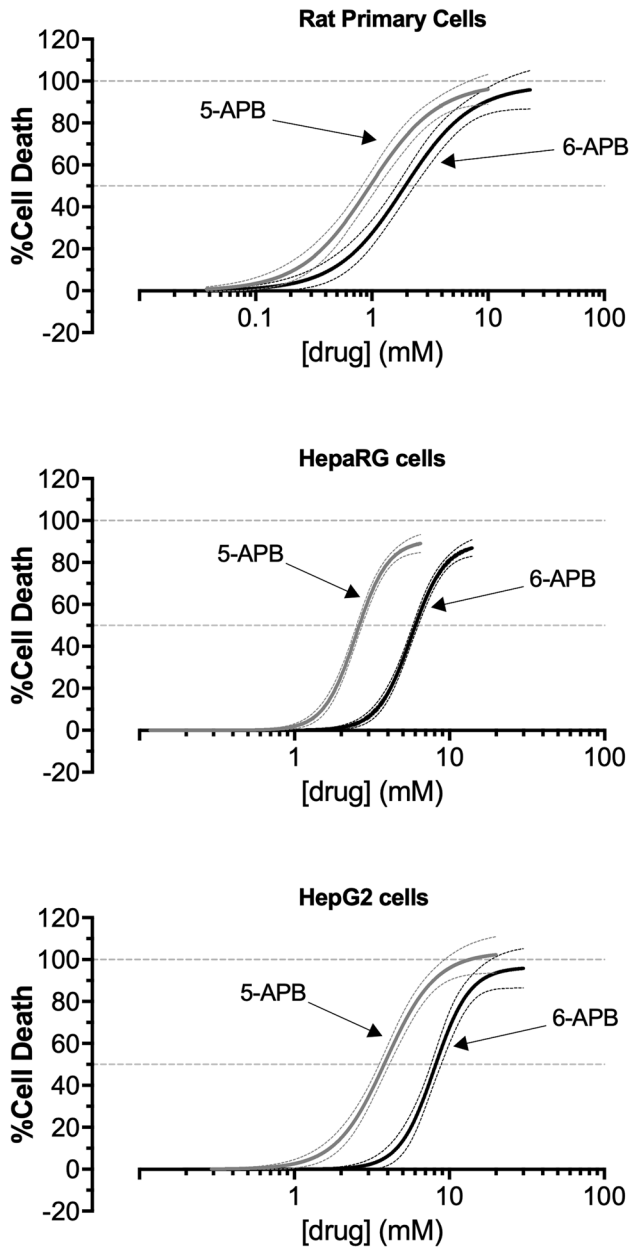

Fig. 2 Toxicity elicited in primary rat hepatocytes, HepaRG differentiated cells, and HepG2 cells after 24-h exposure to 5-(2-aminopropyl)benzofuran (5-APB, purple solid line) and 6-(2-aminopropyl)benzofuran (6-APB, black solid line). Cell viability was assessed by the 3-(4,5-dimethylthiazol-2-yl)-2,5-diphenyltetrazolium bromide (MTT) reduction assay and data are presented as percentage of cell viability relative to the negative controls ($n = 4$). Curves were fitted to the dosimetric Logit model (parameters displayed in Table 2). The dashed lines are the upper and lower limits of the 95% confidence interval of the best estimate of mean responses. The dotted horizontal lines represent 50% and 100% effect

were carried out in primary rat hepatocytes at concentrations that elicited 20, 40, 50, and 70% of cell death (Table 3), as interpolated from the best-fits attained in the MTT assay.

Noteworthy, we also observed the surfacing of intracellular black-brown pigments, following drug incubations at the highest concentrations tested.

Inhibition of CYP isoforms impacts the toxic potential of benzofurans in rat hepatocytes

Cytotoxicity resulting from drug exposure following specific inhibition of CYP2E1, CYP2D6, CYP3A4 or P450 in general is presented in Figs. 3 and 4. These data indicate that inhibition of the different isoforms of P450 led to a decline of the cytotoxicity elicited by 5-APB and 6-APB, as supported by the shift of the concentration–response curves towards the right. By comparing the cytotoxic potencies of the drugs in the presence or absence of the different P450 inhibitors (Table 2), it is also evident that the activities of CYP3A4 and P450, in general, present higher impact on the toxification of both drugs ($p < 0.01$), compared to the effect of CYP2D6 and CYP2E1.

Benzofurans induce oxidative stress in primary rat hepatocytes

Induction of oxidative stress is one of the cornerstone mechanisms of toxicity elicited by classic psychoactive stimulants, such as amphetamines (Dias da Silva et al. 2014a) and cocaine (Martins et al. 2018), but also by more recently emerged club drugs, such as piperazines (Dias da Silva et al. 2015, 2017). We thus determined the role of oxidative stress in the hepatotoxicity elicited by the tested benzofurans by evaluating the formation of ROS/RNS in rat hepatocytes, 24 h after drug exposure. Figure 5 shows that both drugs induced concentration-dependent production of reactive species, and this result was significantly different from controls at concentrations higher than the respective EC_{40} ($p < 0.05$; ANOVA followed by Dunn's test).

In addition, since GSH is a pivotal first-defence against free radicals, we determined the intracellular levels of GSH and GSSG (Fig. 6). All tested concentrations of 5-APB and 6-APB induced a concentration-dependent depletion of GSH, that reached statistical significance at concentrations above the EC_{50} for 5-APB ($p < 0.001$; Kruskal–Wallis test) and above the EC_{40} for 6-APB ($p < 0.05$; Kruskal–Wallis test). The GSSG levels also increased at the EC_{40} and EC_{50} for both benzofurans ($p < 0.01$; Kruskal–Wallis test).

Benzofurans disrupted mitochondrial homeostasis and functioning in primary hepatocytes

Mitochondrial homeostasis was evaluated by measuring the incorporation of the selective probe TMRE in the organelle. Results in Fig. 7 show an increase in $\Delta\psi m$ for both drugs ($p < 0.05$; ANOVA followed by Dunn's test), when

Table 2 Parameters derived from nonlinear fits (asymmetric Logit function) of concentration–mortality data of 5-(aminopropyl)benzofuran (5-APB) and 6-(aminopropyl) benzofuran (6-APB)

	Estimated parameters for the regression model			EC_{50} (mM)	*p* value
	θ_1^a	θ_2^b	θ_{max}^c		
Primary rat hepatocytes					
5-APB	0.07308	3.398	99.09	9.64×10^{-1}	–
5-APB and CYP2D6 inhibitor[d]	− 0.4183	5.034	104.6	1.16×10^{0}	$p = 0.2605$ (vs. no inhibitor)
5-APB and CYP2E1 inhibitor[e]	− 0.3125	6.123	100.6	1.12×10^{0}	$p = 0.1969$ (vs. no inhibitor)
5-APB and CYP3A4 inhibitor[f]	− 1.57	8.271	97.56	1.57×10^{0}	$p < 0.0001$ (vs. no inhibitor)
5-APB and P450 inhibitor[g]	− 0.9326	7.637	100.6	1.32×10^{0}	$p = 0.0047$ (vs. no inhibitor)
6-APB	− 0.9488	3.437	98.17	1.94×10^{0}	$p < 0.0001$(vs. 5-APB)
6-APB and CYP2D6 inhibitor[d]	− 1.547	3.952	107.2	2.28×10^{0}	$p = 0.0118$ (vs. no inhibitor)
6-APB and CYP2E1 inhibitor[e]	− 1.669	3.055	118	2.79×10^{0}	$p = 0.0340$ (vs. no inhibitor)
6-APB and CYP3A4 inhibitor[f]	− 5,335	9.368	98.46	3.74×10^{0}	$p < 0.0001$ (vs. no inhibitor)
6-APB and P450 inhibitor[g]	− 2.651	5.641	102.4	2.89×10^{0}	$p < 0.0001$ (vs. no inhibitor)
HepaRG immortalized human cells					
5-APB	− 3.825	9.650	90.66	2.62×10^{0}	–
6-APB	− 6.957	9.234	89.25	6.02×10^{0}	p <0.0001(vs. 5-APB)
HepG2 immortalized human cells					
5-APB	− 3.645	6.181	103.6	3.79×10^{0}	–
6-APB	− 7.973	8.815	96.45	8.18×10^{0}	p <0.0001(vs. 5-APB)

Data were assessed by the 3-(4,5-dimethylthiazol-2-yl)-2,5-diphenyltetrazolium bromide (MTT) reduction assay, after 24-h incubations, at 37 °C, in cultured primary rat hepatocytes, HepG2 cells or HepaRG differentiated cells (Fig. 2)

[a]Location parameter

[b]Slope parameter

[c]Maximal effect, expressed as % cell death

[d]Quinidine at 10 µM

[e]Metyrapone at 500 µM

[f]Ketoconazole at 1 µM

[g]1-Aminobenzotriazole (1-ABT) at 1 mM. EC_{50}: concentration producing 50% maximal effect (mM)

Table 3 Concentrations (µM) tested for evaluating mechanisms underlying hepatotoxicity of 5-(2-aminopropyl)benzofuran (5-APB) and 6-(2-aminopropyl)benzofuran (6-APB) when primary rat hepatocytes were exposed to the drugs for 24 h at 37 °C

	5-APB (µM)	6-APB (µM)
EC_{20}	5.87×10^{2}	9.33×10^{2}
EC_{40}	1.05×10^{3}	2.05×10^{3}
EC_{50}	1.33×10^{3}	2.74×10^{3}
EC_{70}	2.15×10^{3}	4.58×10^{3}

EC*x*: concentration (µM) producing *x* % of the maximal effect in the 3-(4,5-dimethylthiazol-2-yl)-2,5-diphenyltetrazolium bromide (MTT) assay

compared to control conditions, that was solely reverted at the highest concentration tested (EC_{70}).

Since Δψm is a vital component of the electrochemical proton motive force that drives energy generation by mitochondria, we also determined the intracellular ATP levels. ATP is essential for cells to successfully carry out their energy-dependent functions and, consequently, to survive. Under our experimental conditions, 5-APB and 6-APB significantly impaired cell energetics for all concentrations tested ($p < 0.05$; ANOVA followed by Dunn's test), as depicted in Fig. 8.

Benzofurans activated upstream and downstream apoptotic events that ultimately may render primary hepatocytes to necrosis

The activation of caspase cysteine–aspartic proteases is a hallmark of apoptotic programmed cell death. Figure 9 displays results obtained for the activation of initiator caspase-8 and -9 and executioner caspase-3, following 24-h exposure to 5-APB and 6-APB. Our data show that all treatments led to the activation of upstream and downstream apoptotic pathways, as evidenced by activation of caspases-8, -9, and

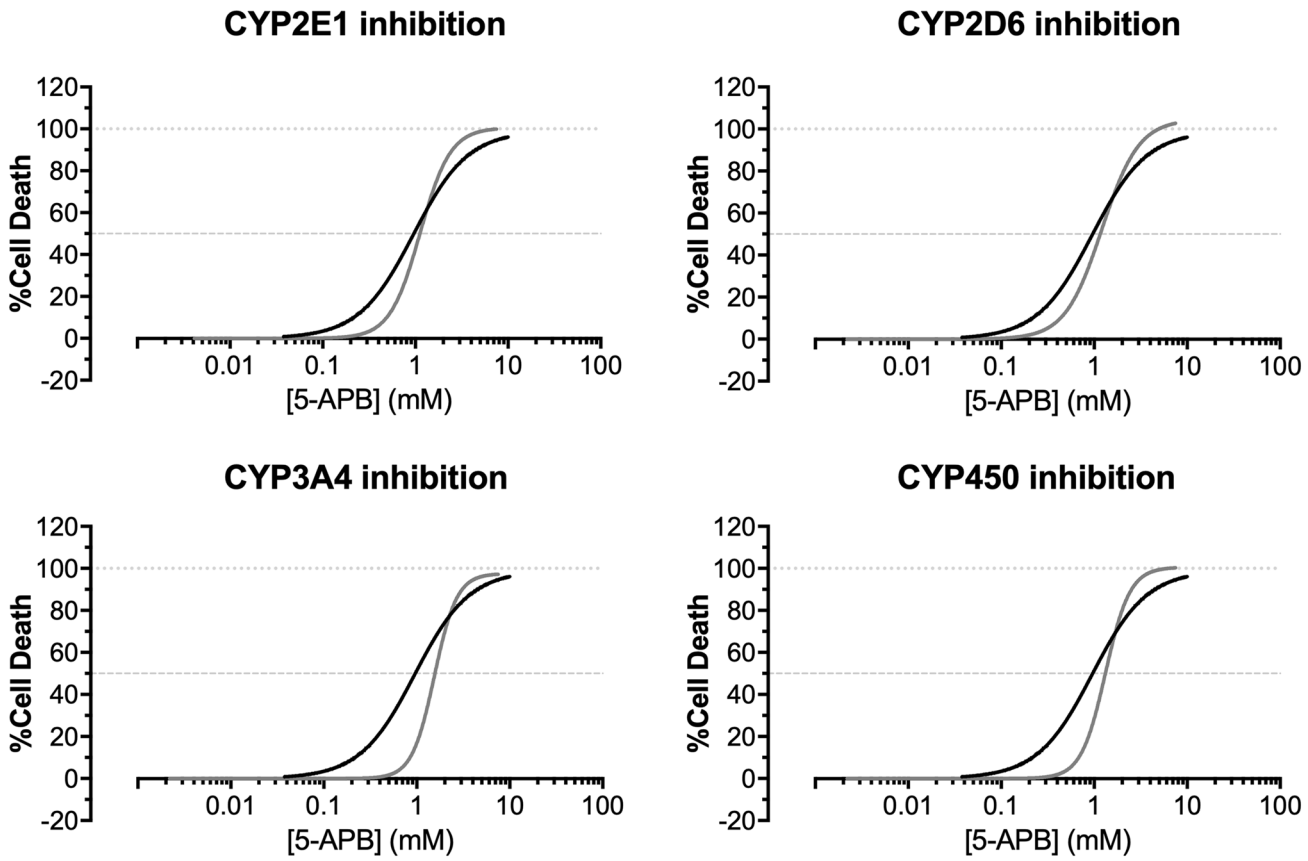

Fig. 3 Toxicity elicited in primary rat hepatocytes after 24-h exposure to 5-(2-aminopropyl)benzofuran (5-APB), following inhibition of CYP2E1, CYP2D6, CYP3A4 or P450 in general. Cell viability was assessed by the 3-(4,5-dimethylthiazol-2-yl)-2,5-diphenyltetrazolium bromide (MTT) reduction assay and data from incubations with (grey solid line) or without (black solid line) inhibitor are presented as percentage of cell viability relative to the negative controls ($n=4$). Curves were fitted to the dosimetric Logit model (parameters displayed in Table 2). The dotted lines represent 50% and 100% effect

-3 ($p<0.05$; ANOVA followed by Dunn's test); the exception was 6-APB at EC_{20} for caspase-3. All the effects were more exacerbated for 5-APB, as compared with 6-APB.

To further clarify the cell death mode, either by necrosis and/or apoptosis, we performed the Hoechst 33342/PI staining of primary rat hepatocytes exposed to 5-APB and 6-APB for a period of 24 h at 37 °C. As depicted in Fig. 10, nuclei in control cells (Fig. 10a) display regular contours and have a large and round size. Early apoptotic events (pyknotic nuclei lacking PI labelling, marked with green arrowheads) can be identified in 6-APB EC_{20} and EC_{40} (Fig. 10c, e) and 5-APB EC_{40} and EC_{70} (Fig. 10d, h). Late apoptotic cells (red condensed nuclei, marked with orange arrowheads) are present in images from all treatments, and necrotic cells (red large nuclei, marked with red arrowheads) in significant numbers in Fig. 10h (5-APB EC_{70}) and g, i (6-APB EC_{50} and EC_{70}, respectively).

Intact cell membrane is also a classical feature of apoptotic cells, while membrane leakage is often considered a typical necrotic feature. Results of LDH leakage in primary rat hepatocytes, shown in Fig. 11, evidenced that both drugs were capable of inducing concentration-dependent damage to cytoplasmic membrane integrity with consequent LDH leakage, in accordance with the Hoechst 33342/PI staining data.

Benzofurans induce autophagy in primary rat hepatocytes

To date there are no reports of autophagy induced by psychoactive benzofurans. Exposure of primary rat hepatocytes to different effect concentrations of 5-APB and 6-APB for 24 h, at 37 °C, induced morphological changes, as observed by phase contrast microscopy, which included a marked increase in cytoplasmic vacuolization (a typical feature of autophagy). Acridine orange was further employed to substantiate the presence of AVO. As expected, acridine orange labelling evidenced the presence

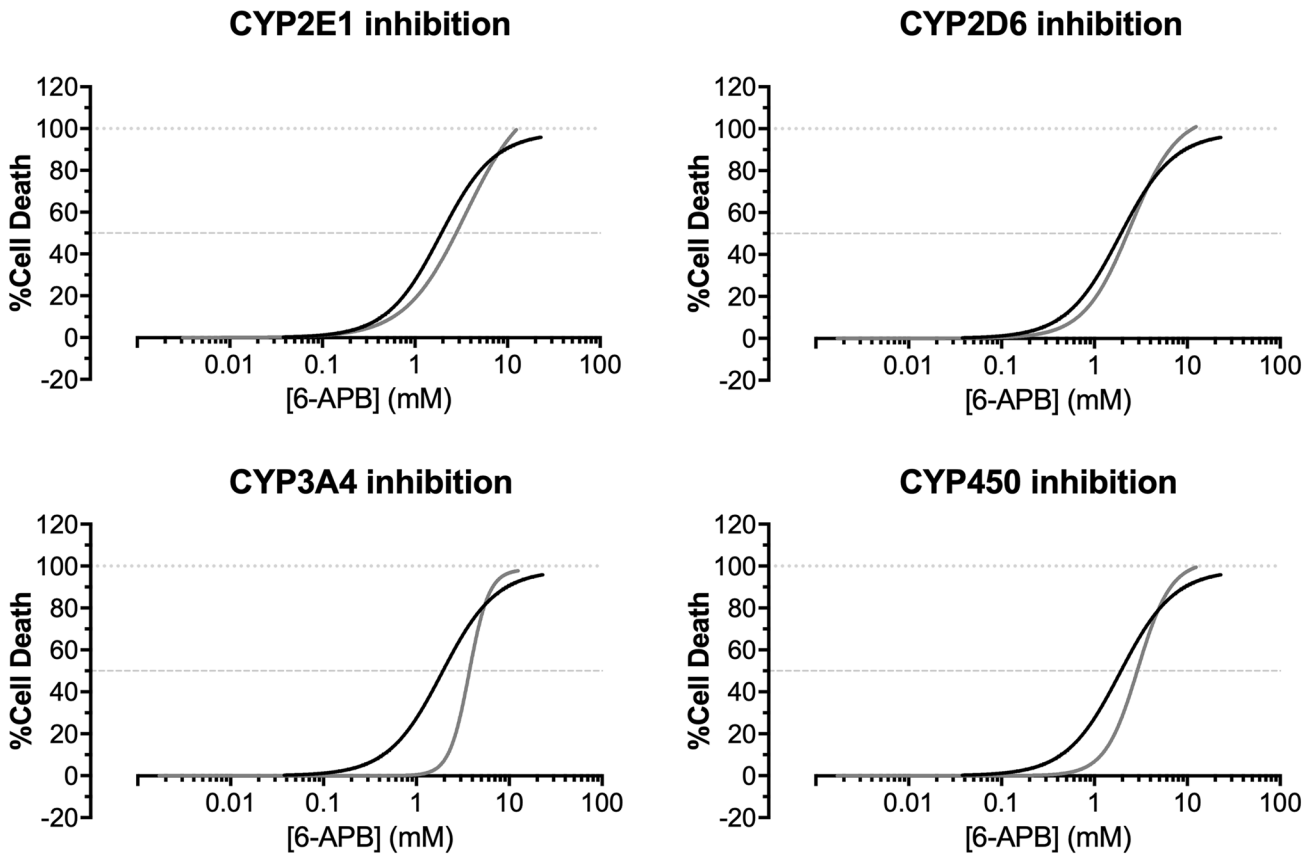

Fig. 4 Toxicity elicited in primary rat hepatocytes after 24-h exposure to 6-(2-aminopropyl)benzofuran (6-APB), following inhibition of CYP2E1, CYP2D6, CYP3A4 or P450 in general. Cell viability was assessed by the 3-(4,5-dimethylthiazol-2-yl)-2,5-diphenyltetrazolium bromide (MTT) reduction assay and data from incubations with (grey solid line) or without (black solid line) inhibitor are presented as percentage of cell viability relative to the negative controls ($n=4$). Curves were fitted to the dosimetric Logit model (parameters displayed in Table 2). The dotted lines represent 50% and 100% effect

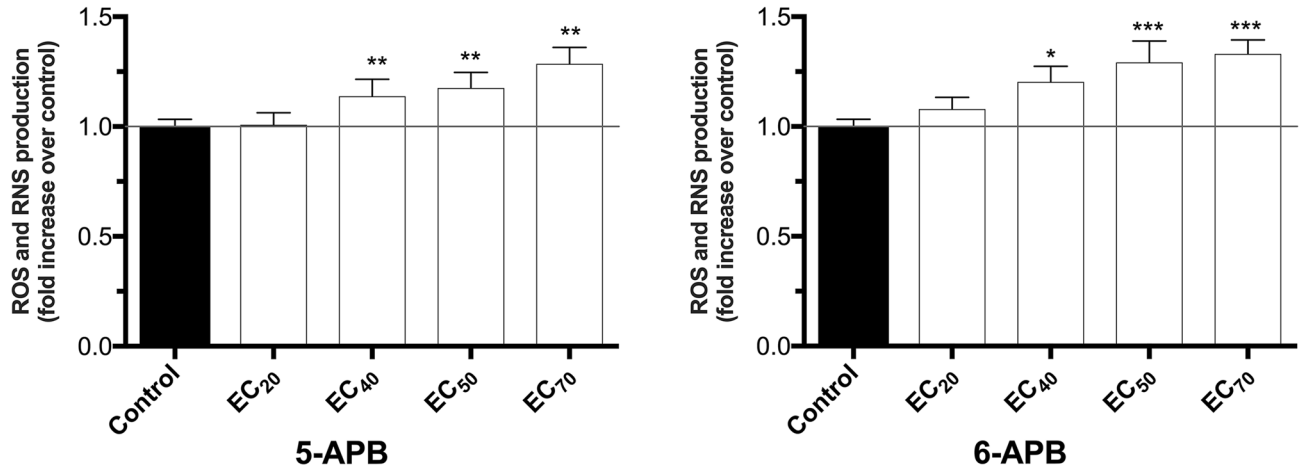

Fig. 5 Production of reactive oxygen (ROS) and nitrogen (RNS) species in primary rat hepatocytes, after exposure to the EC_{20}, EC_{40}, EC_{50}, and EC_{70} of 5-(2-aminopropyl)benzofuran (5-APB) and 6-(2-aminopropyl)benzofuran (6-APB) for 24 h, at 37 °C. Fluorescence data from the 2′,7′-dichlorodihydrofluorescein diacetate (DCFH-DA) assay were normalized to negative controls (no drug exposure, set to 1) and were from five independent experiments. *$p<0.05$, **$p<0.01$, **$p<0.001$; compared to controls. Statistical analysis of data was performed using one-way ANOVA followed by Dunn's multiple comparison test

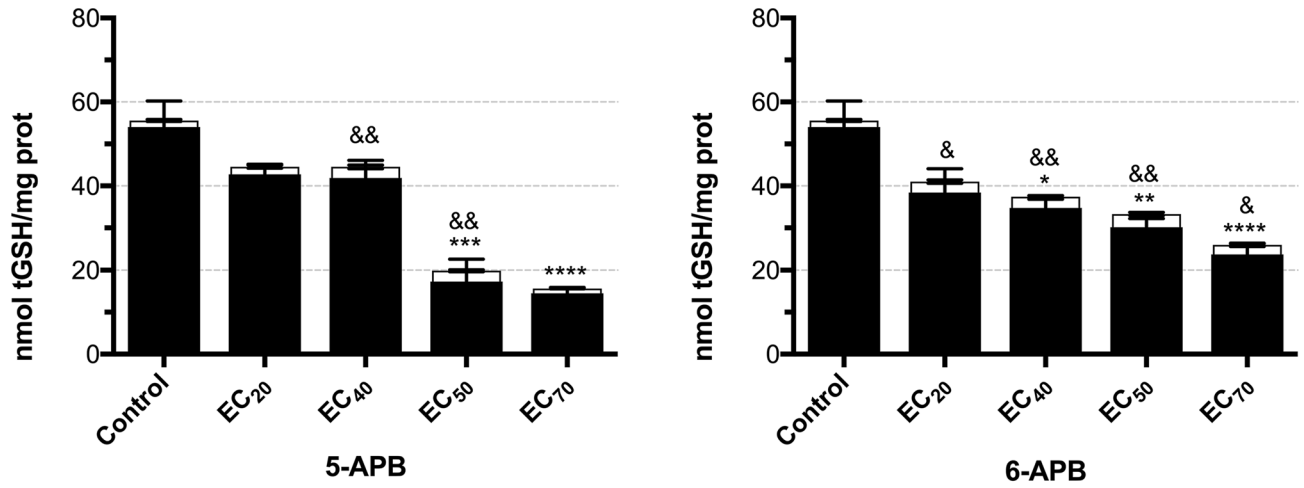

Fig. 6 Intracellular levels of total (tGSH), reduced (GSH; back bars) and oxidized (GSSG; white bars) glutathione in primary rat hepatocytes, after exposure to the EC_{20}, EC_{40}, EC_{50}, and EC_{70} of 5-(2-aminopropyl)benzofuran (5-APB) and 6-(2-aminopropyl)benzofuran (6-APB) for 24 h, at 37 °C. Results were from three independent experiments. $*p<0.05$, $**p<0.01$, $***p<0.001$, $****p<0.0001$; compared to GSH in control. $\&p<0.05$, $\&\&p<0.01$; compared to GSSG in control. Statistical analysis of data was performed using Kruskal–Wallis test

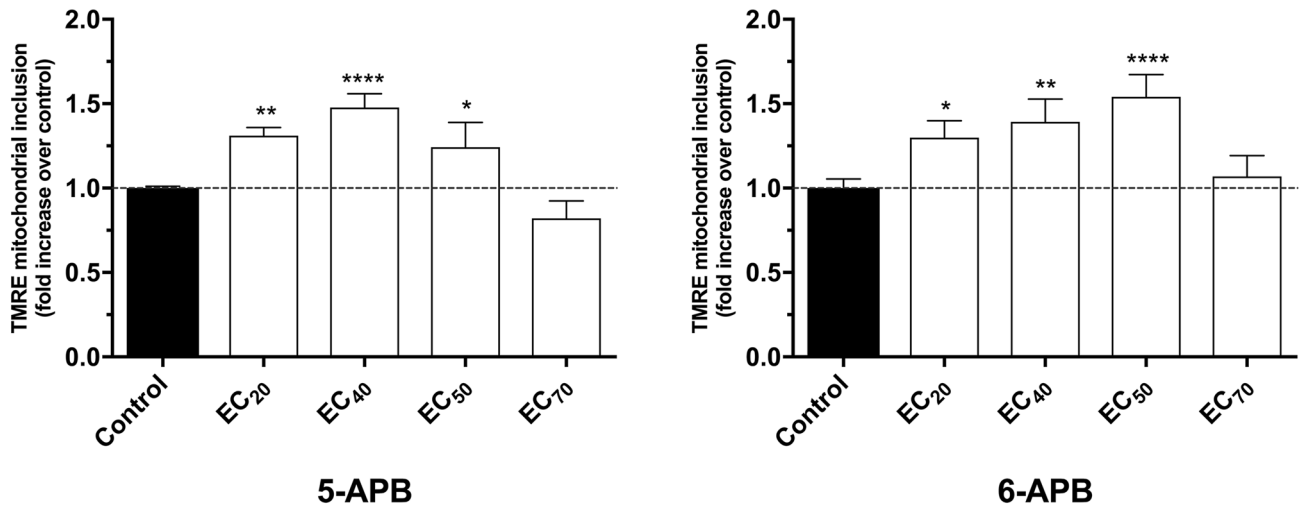

Fig. 7 Mitochondrial membrane potential (ΔΨm) measured by TMRE inclusion assay in primary rat hepatocytes, after exposure to the EC_{20}, EC_{40}, EC_{50}, and EC_{70} of 5-(2-aminopropyl)benzofuran (5-APB) and 6-(2-aminopropyl)benzofuran (6-APB) for 24 h, at 37 °C. Data from five independent experiments were normalized to control conditions (no drug exposure, set to 1). $*p<0.05$, $**p<0.01$, $****p<0.0001$; compared to control. Statistical analysis of data was performed using one-way ANOVA followed by Dunn's multiple comparison test

of a larger amount of acidic vesicles following exposure to EC_{40} of 5-APB and 6-APB (Fig. 12c, e); these are located around the nuclei, as highlighted by pink arrowheads in phase contrast images (Fig. 12d, f).

Discussion

The benzofurans 5-APB and 6-APB, currently unscheduled in several European and US countries, are psychoactive substances with stimulant and entactogenic properties similar to those of amphetamines and, based on the results herein presented, also display similar toxicological mechanisms

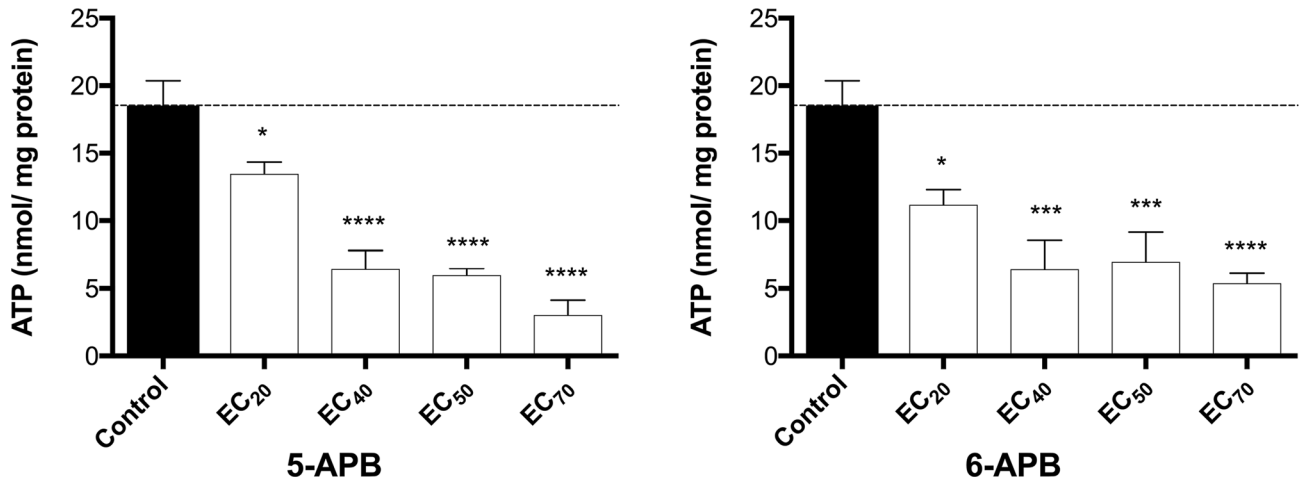

Fig. 8 Intracellular adenosine triphosphate (ATP) levels in primary rat hepatocytes, after exposure to the EC_{20}, EC_{40}, EC_{50}, and EC_{70} of 5-(2-aminopropyl)benzofuran (5-APB) and 6-(2-aminopropyl)benzofuran (6-APB) for 24 h, at 37 °C. Results were from three independent experiments. $*p<0.05$, $***p<0.001$, $****p<0.0001$; compared to control. Statistical analysis of data was performed using one-way ANOVA followed by Dunn's multiple comparison test

(Carvalho et al. 1996; Dias da Silva et al. 2014a; Brown and Yamamoto 2003). These mechanisms are barely elucidated, with little or no information pertaining to the toxicological pathways of these NPS towards such an important organ as the liver. Unfortunately, there is a significant lack of descriptive literature on clinical intoxications with these drugs. Nonetheless, clinical hepatotoxicity is a common outcome of other non-psychoactive benzofuran derivatives (Babany et al. 1987; Hautekeete et al. 1995; Jaiswal et al. 2018; Ratz Bravo et al. 2005; Tsuda et al. 2018; Verhovez et al. 2011), which comes in line with our results. Our study is the first comparing the in vitro hepatotoxicity induced by 5-APB and 6-APB. One previous study has already shed some light upon the toxic potential of benzofurans (Nakagawa et al. 2017) by demonstrating that 4 mM 5-APB induced hepatotoxicity by triggering loss of mitochondrial membrane potential, hampering ATP production and increasing ROS to a greater level than that produced by MDMA. Herein, we further contribute towards the knowledge on *benzofury* toxicity by showing similar effects for 6-APB, but with much lower potency, and by unveiling the involvement of apoptosis, necrosis and autophagy in the hepatotoxicity elicited by 5-APB and 6-APB.

Although the concentrations tested here are higher than the levels found in blood of intoxicated patients (from 0.395 nM to 31.96 µM) (Adamowicz et al. 2014; Chan et al. 2013; Krpo et al. 2018; McIntyre et al. 2015; Barcelo et al. 2017), it is well-known that the liver is exposed to concentrations of amphetamine-like stimulants far higher than the concentrations achieved in blood (De Letter et al. 2006; Garcia-Repetto et al. 2003). Considering the aforementioned structural and functional similarities between these drugs, it is reasonable to consider that the same occurs with the benzofurans tested in this work.

Overall, our study demonstrated lower cytotoxicity in immortalized HepG2 cells, compared to HepaRG cells. HepG2 cells are a cell line that expresses very low levels of essential drug-metabolizing enzymes, such as CYP2B6, CYP1A2 and 3A4, which have been described to be involved in the metabolism of amphetamines and other NPS (Aninat et al. 2006; Carvalho et al. 2012; Gerets et al. 2012; Meyer et al. 2012). Although displaying an enzymatic profile more representative of the hepatocyte in vivo, HepaRG cells were also established from a donor that poorly expressed CYP2D6 and CYP2E1 (Gerets et al. 2012), and the putative involvement of these isoforms in the metabolism of the studied compounds is not to be ignored. Therefore, the use of highly metabolically competent primary rat hepatocytes, which display great levels of P450 isoforms absent or present in low amounts in these human-derived cells, for evaluating the toxicity of 5-APB and 6-APB was therefore considered essential to address the flaws presented by the immortalized models. For both substances, the EC_{50} in primary cells was over 2.7-fold lower, supporting the potential relevance of metabolism by P450, as toxicity appears to be magnified with the increased expression/activity of the drug-metabolizing enzymes. This might signify that the hepatotoxic effects may be due not only to the drugs itself, but also to their indirect action through toxic metabolites. Further investigation is required to establish the toxicological profile of *benzofury* metabolites and their comparative toxicity towards the parent drugs.

To validate the hypothesis that significant disparities concerning hepatotoxicity among the employed models may rely

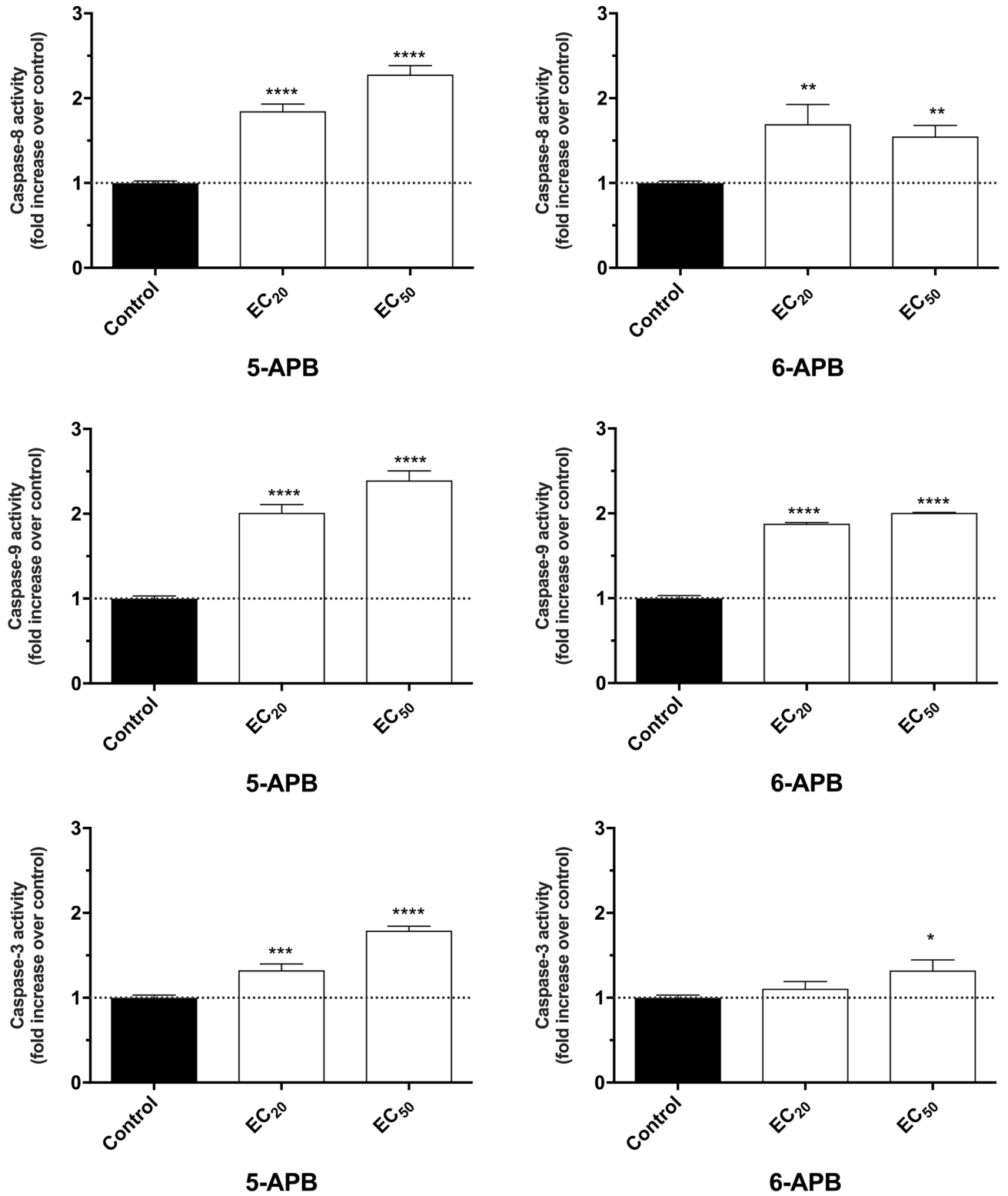

Fig. 9 Caspase-8, -9 and -3 activation in primary rat hepatocytes, after exposure to the EC_{20}, and EC_{50} of 5-(2-aminopropyl)benzofuran (5-APB) and 6-(2-aminopropyl)benzofuran (6-APB) for 24 h, at 37 °C. Results from four independent experiments were normalized to control (no drug exposure, set to 1). $^{*}p<0.05$, $^{**}p<0.01$, $^{***}p<0.001$, $^{****}p<0.0001$; compared to control. Statistical analysis of data was performed using one-way ANOVA followed by Dunn's multiple comparison test

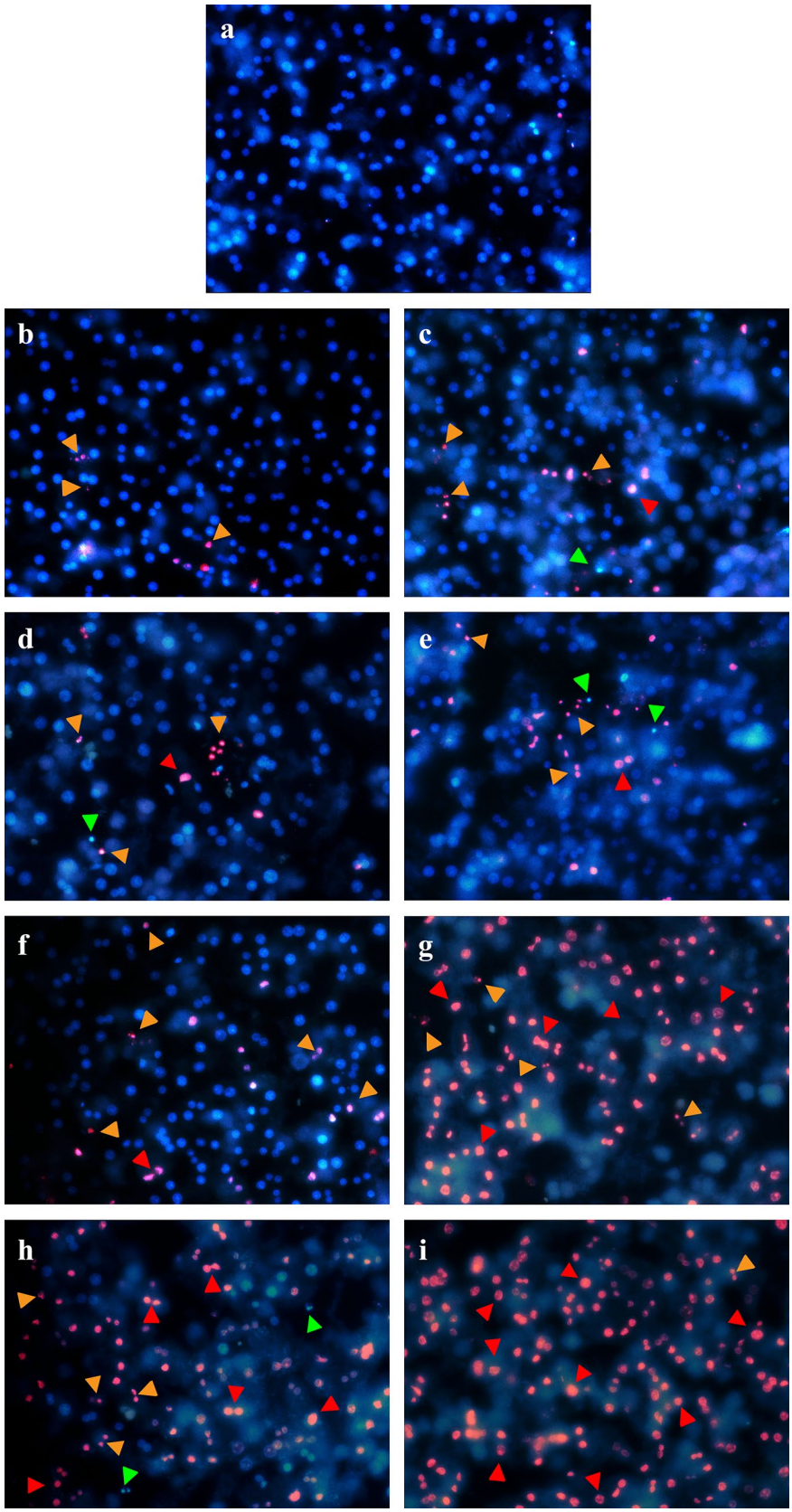

Fig. 10 Representative fluorescence microphotographs of Hoechst 33342/propidium iodide staining of primary rat hepatocytes after exposure to the EC_{20}, EC_{40}, EC_{50}, and EC_{70} of 5-(2-aminopropyl)benzofuran (5-APB) (**b**, **d**, **f**, and **h**, respectively) and 6-(2-aminopropyl)benzofuran (6-APB) (**c**, **e**, **g** and **i**, respectively) for 24 h, at 37 °C. Microphotograph **a** represents control conditions. Red arrows indicate necrotic cells, green arrows indicate early apoptotic cells and orange arrows indicate late apoptotic cells. Original magnification, 200 ×

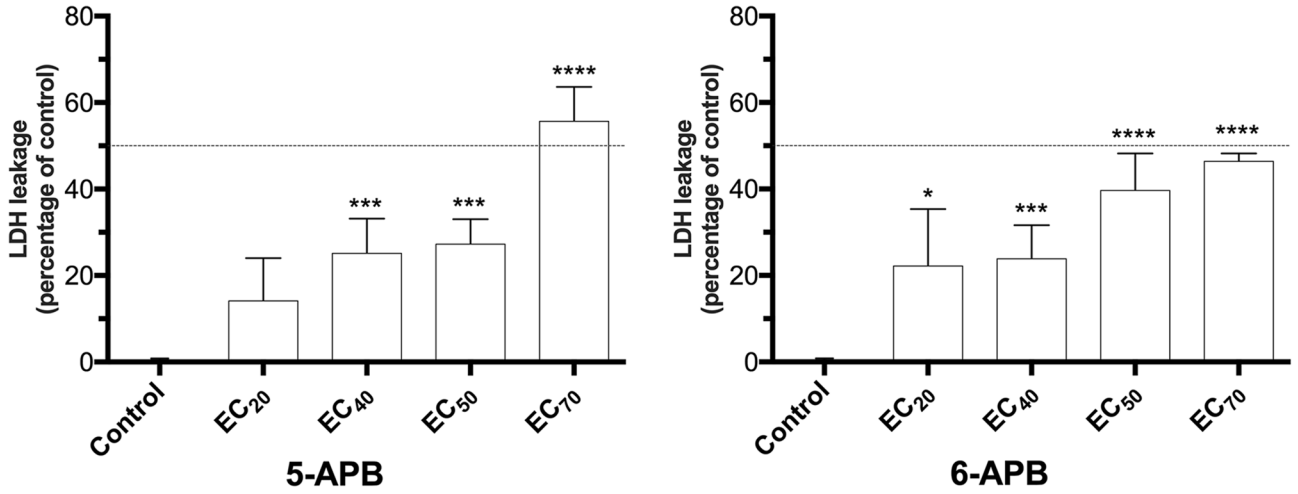

Fig. 11 LDH leakage in primary rat hepatocytes, after exposure to the EC_{20}, EC_{40}, EC_{50}, and EC_{70} of 5-(2-aminopropyl)benzofuran (5-APB) and 6-(2-aminopropyl)benzofuran (6-APB) for 24 h, at 37 °C. Results from four independent experiments were normalized to negative and positive controls (set to 0% and 100%, respectively). $^{*}p < 0.05$, $^{***}p < 0.001$, $^{****}p < 0.0001$; compared to control. Statistical analysis of data was performed using one-way ANOVA followed by Dunn's multiple comparison test

on the activity and/or expression of their P450 isoforms, further experiments employing enzymatic inhibitors were carried out in primary rat hepatocytes, which is the most relevant model in what concerns P450 content. The most important alterations in drug potency occurred following specific inhibition of CYP3A4 and unspecific inhibition of P450, but whether the latter results from CYP3A4 inhibition by the non-specific inhibitor, requires further confirmation. Metabolism of *benzofury* through CYP3A4 may involve an epoxide formation, as furan toxicity has been associated with bioactivation through this enzyme into a highly reactive epoxide, followed by ring opening into an γ-keto aldehyde (Meyer et al. 2012). In accordance, Connelly et al. (2002) reported that 2,3-benzofuran converts to 2-(2-hydroxyphenyl)ethanal via ring cleavage, in Sprague–Dawley rats. Such toxic γ-keto aldehyde intermediates are able to form adducts with cell biomolecules, previous to their urinary excretion (Smith 2011). Previous works pertaining to unveil the metabolism of both 5-APB and 6-APB corroborate this hypothesis by showing that the first step of their metabolic pathway is indeed furan oxidative metabolism through ring cleavage (Welter et al. 2015a, b). Alternatively, the epoxide can ultimately give rise to a lactone that can also form adducts, including with CYP3A4. In fact, a number of furan-containing compounds were described to act as mechanism-based inhibitors of CYP3A4 due to the formation of covalently bonded adducts (Meyer et al. 2012). One previous study with the well-known benzofuran amiodarone and its main metabolite, desethylamiodarone, established that the metabolite caused greater loss of HepG2 viability than the parent compound, the metabolite formation was greatly dependent on CYP3A4, and the abolishment of desethylamiodarone cytotoxicity occurred upon co-exposure of amiodarone with a CYP3A4 inhibitor (Wu et al. 2016). As such, the hypothesis of 5-APB and 6-APB metabolites being more toxic than the parent drugs should not be discarded.

Both CYP2E1 and CYP2D6 inhibitors also decreased the sensitivity of hepatocytes to benzofurans, but to a lesser extent. Dinger et al. (2016) previously identified 6-APB and 5-APB as substrates of CYP2D6, but other studies attempting to establish which CYP isoforms were involved in the metabolic pathways of both drugs did not succeed due to the low rate of metabolite formation (Connelly et al. 2002; Smith 2011). In line with our data, other studies revealed that CYP2D6 inhibition reduced the hepatotoxic potential of some other synthetic stimulants, namely cathinones (Valente et al. 2016; Pedersen et al. 2013), and piperazines (Dias da Silva et al. 2015).

One important finding of our work was the formation of intracellular brown-black pigments following exposure of primary hepatocytes to the highest drug concentrations tested. These pigments had maximal absorbance in the same wavelength range of the formazans and could, therefore, influence the absorbance readings in the MTT viability assay. However, this was not problematic since their formation only occurred at concentrations for which the maximum effect in the assay had already been achieved (higher than 10 mM for 6-APB and 5 mM for 5-APB). Similar findings had already been observed for amphetamines (Dias da Silva et al. 2014b) and were attributed to the production of aminochromes, whose subsequent oxidation leads to the production of melanin-type polymers. These aminochromes are formed through catechol intermediates that oxidize into the corresponding *o*-quinones, which are highly redox active molecules that react with GSH, free

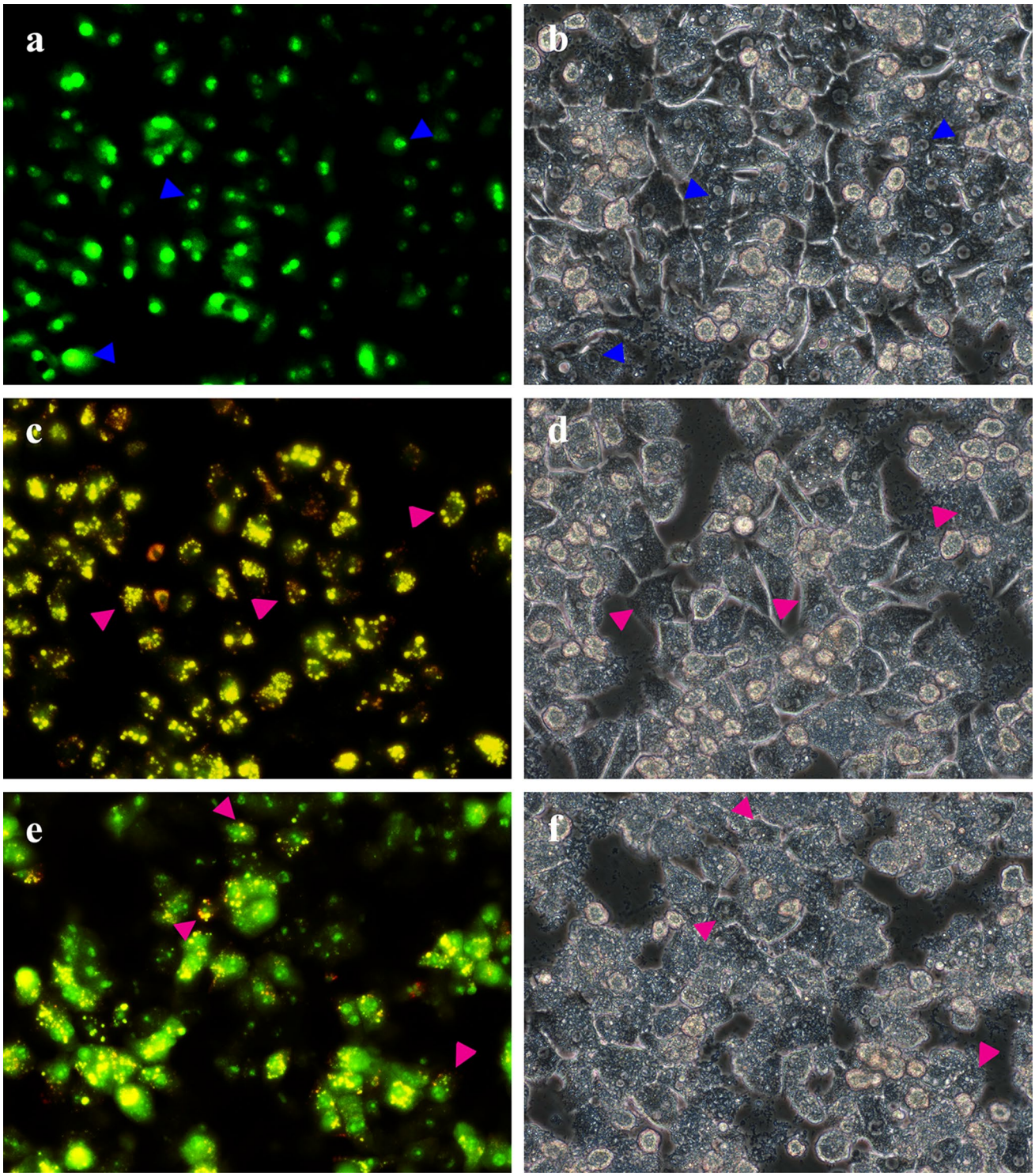

Fig. 12 Representative phase contrast (**b**, **d**, **f**) and fluorescence (**a**, **c**, **e**) microphotographs of primary hepatocytes stained with acridine orange. Cells treated with EC_{40} of 5-APB (**c**, **d**) and EC_{40} of 6-APB (**e**, **f**) for 24 h, at 37 °C, present acidic vesicular organelles stained in orange to red (pink arrow), which are absent in control cells (**a**, **b**). Blue arrows indicate cell nuclei. Original magnification, 200 ×

cysteine and cysteinyl residues on proteins, resulting in significant modification of macromolecules, including proteins, lipids and deoxyribonucleic acid (DNA). Also, *o*-quinones can enter in oxidative cycling, increasing pro-oxidant burst and depleting cell from antioxidant defences (Dias da Silva et al. 2014a). In agreement with these facts, significant

oxidative stress arose from the exposure of hepatocytes to 5-APB and 6-APB, which is also in line with the epoxide formation hypothesis. Previous studies employing non-psychoactive benzofurans such as amiodarone and benzbromarone, developed as treatment for arrhythmia and gout, respectively, showed the benzofuran ability to induce an increase in ROS, as did Nakagawa and co-workers when fresh rat hepatocytes were exposed to 5-APB and its *N*-methylated congener 5-MAPB (Nakagawa et al. 2017; Kaufmann et al. 2005; Waldhauser et al. 2006). Although no catechol or *o*-quinone metabolites have been described for 5-APB and its 6-congener, the increased oxidative stress observed following the exposure of cells to these drugs suggests that the formation of these products should not be excluded. Noteworthy, amiodarone and benzbromarone reportedly led to quinone and catechol formation through hepatic metabolism (McDonald and Rettie 2007; Parmar et al. 2016; Ramesh Varkhede et al. 2014). Importantly, the benzofuran moiety was already identified as liable for the formation of reactive quinones (Parmar et al. 2016). There is one report describing the activation of melanogenesis following exposure to a benzofuran compound, mecinarone, thus supporting the possibility of formation of melanin-like polymers following *benzofury* exposure (Bailly et al. 1981). To further identify the source of these polymers, additional studies should be carried out by isolating the metabolites of 5-APB and 6-APB, exposing primary hepatocytes to each of them, and ultimately characterizing the polymers and adducts formed.

The most noticeable cell defence against reactive species and electrophilic xenobiotics is GSH. The role of this pivotal antioxidant becomes even more important in the liver, a primary target for damage induced by pernicious drugs, much due to the relevance of the drug-metabolizing processes in this organ (Forman et al. 2009; Yuan and Kaplowitz 2013). Of note, amiodarone and usnic acid, another benzofuran-containing molecule, are reported in the literature to cause a diminution of glutathione in mouse hepatocytes (Han et al. 2004; Takai et al. 2016). The significant GSH depletion promoted by 5-APB and 6-APB in the present work is also corroborated by previous experiments in rat hepatocytes with 5-APB and 5-MAPB (Nakagawa et al. 2017) and with amphetamine-related drugs (Dias da Silva et al. 2014a, 2015, 2017), but this effect was not always accompanied by the complementary expected increase in GSSG levels. This can result from the efflux of GSSG into the cell culture medium, which is favoured to defend cells against the disproportionate oxidative stress (Carvalho et al. 1996; Dias da Silva et al. 2014a) but it may also be explained by the formation of conjugates of GSH with reactive metabolites, resembling what occurs with amphetamines (Carvalho et al. 1996; Hiramatsu et al. 1990; Monks et al. 2004).

Furthermore, our data also substantiate the ability of benzofurans to interfere with mitochondrial homeostasis, by impacting $\Delta\psi m$ and cell energetics. Hinder of ATP production had previously been reported for non-psychoactive benzofurans (Kaufmann et al. 2005; Waldhauser et al. 2006). Although the ATP decline confirms results from previous works with MDMA (Dias da Silva et al. 2014a) and synthetic cathinones (Valente et al. 2016; Dias da Silva et al. 2019), the apparent mitochondria hyperpolarization was unexpected, since a decrease of mitochondrial membrane potential often occurred for other related stimulants, as well as for 5-APB in a previous work (Nakagawa et al. 2017). However, Nakagawa and colleagues only assessed alterations to the $\Delta\psi m$ for 4 mM 5-APB; at this concentration level, our results also suggest a decrease of $\Delta\psi m$ for 5-APB. Hyperpolarization of the mitochondrial membrane was previously registered after cardiomyocyte exposure to cocaine and ethanol (Martins et al. 2018), as well as in neurons exposed to piperazines (Arbo et al. 2016). It may be possible to explain this occurrence when considering that the TMRE assay is susceptible to changes brought upon by dysregulation of intracellular ionic charges (such as calcium release from mitochondrial and endoplasmic reticulum stores) which, in turn, can cause an increase in $\Delta\psi m$ (Perry et al. 2011). Further assays to evaluate intracellular calcium levels of the hepatocyte would be essential to confirm whether this is also the case for benzofurans.

Mitochondrial hyperpolarization was previously described to induce caspase activation and chromatin condensation (Griffiths and Rutter 2009). In this line, mitochondria are also dynamic organelles in regulating the intracellular signalling programme that mediates apoptosis. All pathways of apoptosis converge upon the activation of proteases, such as caspase-3, which orchestrate the efficient cell dismantling. Our experimental data evidences that 5-APB and 6-APB trigger the two main pathways leading to caspase activation: the extrinsic route initiated by cell surface receptors leading directly to caspase 8 activation, and the intrinsic pathway that is regulated by mitochondria through activation of caspase-9. Both extrinsic and intrinsic apoptotic pathways converge to activate caspase-3, whose proteolytic activity leads to a cascade of events that culminate in the execution of programmed cell death. Activation of the initiator caspases elicited by both benzofurans is greater than that observed for caspase-3 activity, and 5-APB seems to more efficiently impact the activity of these proteases than 6-APB. Similarly, caspase-3 activation has been previously demonstrated for MDMA (Dias da Silva et al. 2013a; Montiel-Duarte et al. 2002), along with caspase-8 and -9 activation for cathinones (Valente et al. 2016; Dias da Silva et al. 2019) and piperazines (Dias da Silva et al. 2015) in rat hepatocytes. Apoptosis triggered by activation of initiator and effector caspases is also corroborated by the results of the Hoechst/PI staining, which show condensation of nuclei chromatin (Ormerod et al. 1993). Apoptosis (Kaufmann et al. 2005; Chen et al. 2018; Liu et al. 2016),

as well as necrosis (Waldhauser et al. 2006; Han et al. 2004; McMurtry and Mitchell 1977) have been reported following benzofuran exposure in hepatic cell lines (HepG2), isolated rat and mouse hepatocytes and human chondrosarcoma cells.

The concentration-dependent LDH leakage observed for 5-APB and 6-APB had been also previously described for D-amphetamine, MDMA and a few synthetic cathinones in rat hepatocytes (Valente et al. (2016); Beitia et al. 1999; El-Tawil et al. 2011), and can be related with the progression of apoptotic events through a phenomenon designated secondary necrosis (Zhang et al. 2018). Accordingly, during apoptosis, if hepatocytes are not scavenged, they progress to a programmed lytic phase, in which extrinsic pathway-activated caspase-3 may cleave gasdermin D-related protein DFNA5, generating necrotic DFNA5 N-terminal fragment that forms oligomers and transits to the plasmatic membrane wherein it triggers the formation of non-selective pores and consequently leads to the rupture of the membrane integrity. In the case of 5-APB, the observed LDH leakage is compatible with the significant increase in activation of initiator caspase-8 and effector caspase-3, and with cell morphological features indicative of necrosis. For 6-APB, the activation of effector caspase occurs at higher levels than those verified for 5-APB, however marked necrosis in league with the LDH leakage is also at place. While a great number of early and late apoptotic cells was observed at the lower tested concentrations, necrotic events prevail at the concentrations higher than 2.15 mM for 5-APB and 2.74 mM for 6-APB, substantiating drug-induced bimodal cell death, depending on the severity of the injury.

Autophagy is an engulfing process during which obsolete and/or altered cell organelles and proteins are phagocytized and recycled, to maintain the cellular environment in good condition. The process is sparked by various stimuli such as oxidative stress (Navarro-Yepes et al. 2014) and controlled by different signalling pathways. Excessive activation of autophagy can induce apoptosis or necrosis, as well as precipitate cell function shutdown (Galluzzi et al. 2008). Autophagy was previously described following exposure to non-psychoactive benzofurans (Chen et al. 2014; Geng et al. 2018; Hsieh et al. 2015; Lin et al. 2015), but our findings represent the first report of autophagy induced by 5-APB and 6-APB. This homeostatic process was already described in neuronal cells exposed to methamphetamine (Chandramani Shivalingappa et al. 2012; Huang et al. 2017), as well as in liver exposed to alcohol (Schneider and Cuervo 2014). The activation of autophagy described herein also correlates with the observed increase in ROS and RNS, as previously described for other synthetic stimulants (Valente et al. 2017; Chandramani Shivalingappa et al. 2012; Huang et al. 2017).

In conclusion, psychoactive benzofurans are marketed without previous testing for human safety and fallaciously mentioned to be safer than classical stimulants. Notwithstanding, we demonstrated for the first time the concentration-dependent hepatotoxic effects of two benzofurans, 6-APB and 5-APB, in three in vitro models of the hepatocyte. For all models, 5-APB proved to be the most hepatotoxic drug and primary rat hepatocytes displayed highest sensitivity to the toxicity of both drugs. It also became evident that metabolism plays an important part in the toxicity of *benzofury*, and we hypothesize the formation of intermediate epoxide and *o*-quinones that may help explain the marked oxidative stress and dark-brown pigment formation in cell cultures exposed to both drugs. Disruption of redox homeostasis may have interfered with mitochondrial function, resulting in accentuated exhaustion of ATP supplies and in the enhanced activation of cell death pathways, such as caspase-induced apoptosis, necrosis and autophagy. All these toxic mechanisms overlap those of amphetamines and structurally related NPS, including synthetic piperazines and cathinones. The present findings assume great relevance from a scientific perspective, as they advance the knowledge on NPS by clarifying the toxicological mechanisms of other *benzofury* that may yet reach the market; and also from a clinical and forensic perspective as to assist health professionals in the event of intoxicated patients who present themselves to emergency room services after consuming these compounds.

Funding This work was financed by FEDER funds through the COMPETE 2020—Operacional Programme for Competitiveness and Internationalisation (POCI), and by Portuguese funds through FCT—Fundação para a Ciência e a Tecnologia in the framework of the project POCI-01-0145-FEDER-029584. This work was also supported by the Applied Molecular Biosciences Unit—UCIBIO (UID/Multi/04378/2019). To all financing sources the authors are greatly indebted.

Compliance with ethical standards

Conflict of interest The authors declare that they have no conflict of interest.

Ethical approval All applicable international, national, and/or institutional guidelines for the care and use of animals were followed. All procedures performed in studies involving animals were in accordance with the ethical standards of the institution at which the studies were conducted and ethical approval was obtained from the local Ethical Committee for the Welfare of Experimental Animals (University of Porto-ORBEA; project 158/2014) and by the national authority *Direção Geral de Alimentação e Veterinária* (DGAV).

References

ACDM (2013) Benzofurans: A review of the evidence of use and harm. London: Advisory Council on the Misuse of Drugs 2013

Adamowicz P, Zuba D, Byrska B (2014) Fatal intoxication with 3-methyl-N-methylcathinone (3-MMC) and 5-(2-aminopropyl)

benzofuran (5-APB). Forensic Sci Int 245C:126–132. https://doi.org/10.1016/j.forsciint.2014.10.016

Aninat C, Piton A, Glaise D, Le Charpentier T, Langouet S, Morel F et al (2006) Expression of cytochromes P450, conjugating enzymes and nuclear receptors in human hepatoma HepaRG cells. Drug Metab Dispos 34(1):75–83. https://doi.org/10.1124/dmd.105.006759

Arbo MD, Silva R, Barbosa DJ, Dias da Silva D, Silva SP, Teixeira JP et al (2016) In vitro neurotoxicity evaluation of piperazine designer drugs in differentiated human neuroblastoma SH-SY5Y cells. J Appl Toxicol 36(1):121–130. https://doi.org/10.1002/jat.3153

Babany G, Larrey D, Pessayre D, Degott C, Rueff B, Benhamou JP (1987) Chronic active hepatitis caused by benzarone. J Hepatol 5(3):332–335. https://doi.org/10.1016/s0168-8278(87)80039-9

Bailly Y, Oliver C, Raynaud G, Wegmann R (1981) Activation of melanogenesis in the beagle by a vasodilator, mecinarone. Toxicol Eur Res 3(1):45–50

Barcelo B, Gomila I, Rotolo MC, Marchei E, Kyriakou C, Pichini S et al (2017) Intoxication caused by new psychostimulants: analytical methods to disclose acute and chronic use of benzofurans and ethylphenidate. Int J Legal Med 131(6):1543–1553. https://doi.org/10.1007/s00414-017-1648-9

Beitia G, Cobreros A, Sainz L, Cenarruzabeitia E (1999) 3,4-Methylenedioxymethamphetamine (ecstasy)-induced hepatotoxicity: effect on cytosolic calcium signals in isolated hepatocytes. Liver 19(3):234–241. https://doi.org/10.1111/j.1478-3231.1999.tb00041.x

Bouma ME, Rogier E, Verthier N, Labarre C, Feldmann G (1989) Further cellular investigation of the human hepatoblastoma-derived cell line HepG2: morphology and immunocytochemical studies of hepatic-secreted proteins. Vitro Cell Dev Biol. 25(3 Pt 1):267–275

Brown JM, Yamamoto BK (2003) Effects of amphetamines on mitochondrial function: role of free radicals and oxidative stress. Pharmacol Ther 99(1):45–53. https://doi.org/10.1016/S0163-7258(03)00052-4

Carvalho F, Remiao F, Amado F, Domingues P, Correia AJ, Bastos ML (1996) d-Amphetamine interaction with glutathione in freshly isolated rat hepatocytes. Chem Res Toxicol 9(6):1031–1036. https://doi.org/10.1021/tx9501750

Carvalho F, Remiao F, Soares ME, Catarino R, Queiroz G, Bastos ML (1997) d-Amphetamine-induced hepatotoxicity: possible contribution of catecholamines and hyperthermia to the effect studied in isolated rat hepatocytes. Arch Toxicol 71(7):429–436

Carvalho M, Carvalho F, Bastos ML (2001) Is hyperthermia the triggering factor for hepatotoxicity induced by 3,4-methylenedioxymethamphetamine (ecstasy)? An in vitro study using freshly isolated mouse hepatocytes. Arch Toxicol 74(12):789–793

Carvalho M, Carmo H, Costa VM, Capela JP, Pontes H, Remiao F et al (2012) Toxicity of amphetamines: an update. Arch Toxicol 86(8):1167–1231. https://doi.org/10.1007/s00204-012-0815-5

Chan WL, Wood DM, Hudson S, Dargan PI (2013) Acute psychosis associated with recreational use of benzofuran 6-(2-aminopropyl)benzofuran (6-APB) and cannabis. J Med Toxicol. 9(3):278–281. https://doi.org/10.1007/s13181-013-0306-y

Chandramani Shivalingappa P, Jin H, Anantharam V, Kanthasamy A, Kanthasamy A (2012) N-acetyl cysteine protects against methamphetamine-induced dopaminergic neurodegeneration via modulation of redox status and autophagy in dopaminergic cells. Parkinsons Dis 2012:424285. https://doi.org/10.1155/2012/424285

Chen S, Dobrovolsky VN, Liu F, Wu Y, Zhang Z, Mei N et al (2014) The role of autophagy in usnic acid-induced toxicity in hepatic cells. Toxicol Sci 142(1):33–44. https://doi.org/10.1093/toxsci/kfu154

Chen S, Ren Z, Yu D, Ning B, Guo L (2018) DNA damage-induced apoptosis and mitogen-activated protein kinase pathway contribute to the toxicity of dronedarone in hepatic cells. Environ Mol Mutagen 59(4):278–289. https://doi.org/10.1002/em.22173

Clemente CG, Chiappini S, Claridge H, Goodair C, Loi B (2012) Deaths involving 'Benzo Fury', United Kingdom, 2011–2012. International Centre for Drug Policy. University of London, St George's

Connelly JC, Connor SC, Monte S, Bailey NJ, Borgeaud N, Holmes E et al (2002) Application of directly coupled high performance liquid chromatography-NMR-mass spectrometry and 1H NMR spectroscopic studies to the investigation of 2,3-benzofuran metabolism in Sprague-Dawley rats. Drug Metab Dispos 30(12):1357–1363. https://doi.org/10.1124/dmd.30.12.1357

De Letter EA, Piette MH, Lambert WE, Cordonnier JA (2006) Amphetamines as potential inducers of fatalities: a review in the district of Ghent from 1976–2004. Med Sci Law 46(1):37–65. https://doi.org/10.1258/rsmmsl.46.1.37

Dias da Silva D, Carmo H, Lynch A, Silva E (2013a) An insight into the hepatocellular death induced by amphetamines, individually and in combination: the involvement of necrosis and apoptosis. Arch Toxicol 87(12):2165–2185. https://doi.org/10.1007/s00204-013-1082-9

Dias da Silva D, Carmo H, Silva E (2013b) The risky cocktail: what combination effects can we expect between ecstasy and other amphetamines? Arch Toxicol 87(1):111–122. https://doi.org/10.1007/s00204-012-0929-9

Dias da Silva D, Silva E, Carmo H (2013c) Cytotoxic effects of amphetamine mixtures in primary hepatocytes are severely aggravated under hyperthermic conditions. Toxicol In Vitro 27(6):1670–1678. https://doi.org/10.1016/j.tiv.2013.04.010

Dias da Silva D, Silva E, Carmo H (2014a) Combination effects of amphetamines under hyperthermia—the role played by oxidative stress. J Appl Toxicol 34(6):637–650. https://doi.org/10.1002/jat.2889

Dias da Silva D, Silva E, Carvalho F, Carmo H (2014b) Mixtures of 3,4-methylenedioxymethamphetamine (ecstasy) and its major human metabolites act additively to induce significant toxicity to liver cells when combined at low, non-cytotoxic concentrations. J Appl Toxicol 34(6):618–627. https://doi.org/10.1002/jat.2885

Dias da Silva D, Arbo MD, Valente MJ, Bastos ML, Carmo H (2015) Hepatotoxicity of piperazine designer drugs: Comparison of different in vitro models. Toxicol In Vitro 29(5):987–996. https://doi.org/10.1016/j.tiv.2015.04.001

Dias da Silva D, Silva MJ, Moreira P, Martins MJ, Valente MJ, Carvalho F et al (2017) In vitro hepatotoxicity of 'Legal X': the combination of 1-benzylpiperazine (BZP) and 1-(m-trifluoromethylphenyl)piperazine (TFMPP) triggers oxidative stress, mitochondrial impairment and apoptosis. Arch Toxicol 91(3):1413–1430. https://doi.org/10.1007/s00204-016-1777-9

Dias da Silva D, Ferreira B, Roque Bravo R, Rebelo R, Duarte de Almeida T, Valente MJ, Silva JP, Carvalho F, Bastos ML, Carmo H (2019) The new psychoactive substance 3-methylmethcathinone (3-MMC or metaphedrone) induces oxidative stress, apoptosis, and autophagy in primary rat hepatocytes at human-relevant concentrations. Arch Toxicol 93(9):2617–2634

Dinger J, Meyer MR, Maurer HH (2016) In vitro cytochrome P450 inhibition potential of methylenedioxy-derived designer drugs studied with a two-cocktail approach. Arch Toxicol 90(2):305–318. https://doi.org/10.1007/s00204-014-1412-6

El-Tawil OS, Abou-Hadeed AH, El-Bab MF, Shalaby AA (2011) d-Amphetamine-induced cytotoxicity and oxidative stress in isolated rat hepatocytes. Pathophysiology 18(4):279–285. https://doi.org/10.1016/j.pathophys.2011.04.001

EMCDDA (2018) European Drug Report: Trends and development. Luxembourg: European Monitoring Centre for Drugs and Drug Addiction 2018 June 2018. Report No.: 2314-9086

Forman HJ, Zhang H, Rinna A (2009) Glutathione: overview of its protective roles, measurement, and biosynthesis. Mol Aspects Med 30(1–2):1–12. https://doi.org/10.1016/j.mam.2008.08.006

Galluzzi L, Vicencio JM, Kepp O, Tasdemir E, Maiuri MC, Kroemer G (2008) To die or not to die: that is the autophagic question. Curr Mol Med 8(2):78–91. https://doi.org/10.2174/156652408783769616

Garcia-Repetto R, Moreno E, Soriano T, Jurado C, Gimenez MP, Menendez M (2003) Tissue concentrations of MDMA and its metabolite MDA in three fatal cases of overdose. Forensic Sci Int 135(2):110–114. https://doi.org/10.1016/s0379-0738(03)00179-8

Geng X, Zhang X, Zhou B, Zhang C, Tu J, Chen X et al (2018) Usnic acid induces cycle arrest, apoptosis, and autophagy in gastric cancer cells in vitro and in vivo. Med Sci Monit 24:556–566. https://doi.org/10.12659/msm.908568

Gerets HH, Tilmant K, Gerin B, Chanteux H, Depelchin BO, Dhalluin S et al (2012) Characterization of primary human hepatocytes, HepG2 cells, and HepaRG cells at the mRNA level and CYP activity in response to inducers and their predictivity for the detection of human hepatotoxins. Cell Biol Toxicol 28(2):69–87. https://doi.org/10.1007/s10565-011-9208-4

Griffiths EJ, Rutter GA (2009) Mitochondrial calcium as a key regulator of mitochondrial ATP production in mammalian cells. Biochim Biophys Acta 1787(11):1324–1333. https://doi.org/10.1016/j.bbabio.2009.01.019

Guillouzo A, Corlu A, Aninat C, Glaise D, Morel F, Guguen-Guillouzo C (2007) The human hepatoma HepaRG cells: a highly differentiated model for studies of liver metabolism and toxicity of xenobiotics. Chem Biol Interact 168(1):66–73. https://doi.org/10.1016/j.cbi.2006.12.003

Han D, Matsumaru K, Rettori D, Kaplowitz N (2004) Usnic acid-induced necrosis of cultured mouse hepatocytes: inhibition of mitochondrial function and oxidative stress. Biochem Pharmacol 67(3):439–451. https://doi.org/10.1016/j.bcp.2003.09.032

Hautekeete ML, Henrion J, Naegels S, DeNeve A, Adler M, Deprez C et al (1995) Severe hepatotoxicity related to benzarone: a report of three cases with two fatalities. Liver 15(1):25–29

Helander A, Beck O, Backberg M (2015) Intoxications by the dissociative new psychoactive substances diphenidine and methoxphenidine. Clin Toxicol (Phila) 53(5):446–453. https://doi.org/10.3109/15563650.2015.1033630

Hiramatsu M, Kumagai Y, Unger SE, Cho AK (1990) Metabolism of methylenedioxymethamphetamine: formation of dihydroxymethamphetamine and a quinone identified as its glutathione adduct. J Pharmacol Exp Ther 254(2):521–527

Hofer KE, Faber K, Muller DM, Hauffe T, Wenger U, Kupferschmidt H et al (2017) Acute toxicity associated with the recreational use of the novel psychoactive benzofuran N-methyl-5-(2 aminopropyl)benzofuran. Ann Emerg Med 69(1):79–82. https://doi.org/10.1016/j.annemergmed.2016.03.042

Hsieh SL, Chen CT, Wang JJ, Kuo YH, Li CC, Hsieh LC et al (2015) Sedanolide induces autophagy through the PI3K, p53 and NF-kappaB signaling pathways in human liver cancer cells. Int J Oncol 47(6):2240–2246. https://doi.org/10.3892/ijo.2015.3206

Huang YN, Yang LY, Wang JY, Lai CC, Chiu CT, Wang JY (2017) L-ascorbate protects against methamphetamine-induced neurotoxicity of cortical cells via inhibiting oxidative stress, autophagy, and apoptosis. Mol Neurobiol 54(1):125–136. https://doi.org/10.1007/s12035-015-9561-z

Iversen L, Gibbons S, Treble R, Setola V, Huang XP, Roth BL (2013) Neurochemical profiles of some novel psychoactive substances. Eur J Pharmacol 700(1–3):147–151. https://doi.org/10.1016/j.ejphar.2012.12.006

Jaiswal P, Attar BM, Yap JE, Devani K, Jaiswal R, Wang Y et al (2018) Acute liver failure with amiodarone infusion: a case report and systematic review. J Clin Pharm Ther 43(1):129–133. https://doi.org/10.1111/jcpt.12594

Jebadurai J, Schifano F, Deluca P (2013) Recreational use of 1-(2-naphthyl)-2-(1-pyrrolidinyl)-1-pentanone hydrochloride (NRG-1), 6-(2-aminopropyl) benzofuran (benzofury/6-APB) and NRG-2 with review of available evidence-based literature. Hum Psychopharmacol 28(4):356–364. https://doi.org/10.1002/hup.2302

Kaufmann P, Torok M, Hanni A, Roberts P, Gasser R, Krahenbuhl S (2005) Mechanisms of benzarone and benzbromarone-induced hepatic toxicity. Hepatology 41(4):925–935. https://doi.org/10.1002/hep.20634

Krpo M, Luytkis HC, Haneborg AM, Hoiseth G (2018) A fatal blood concentration of 5-APB. Forensic Sci Int 291:e1–e3. https://doi.org/10.1016/j.forsciint.2018.08.044

Lin CW, Chen YS, Lin CC, Chen YJ, Lo GH, Lee PH et al (2015) Amiodarone as an autophagy promoter reduces liver injury and enhances liver regeneration and survival in mice after partial hepatectomy. Sci Rep 5:15807. https://doi.org/10.1038/srep15807

Liu JF, Chen CY, Chen HT, Chang CS, Tang CH (2016) BL-038, a Benzofuran Derivative, Induces Cell Apoptosis in Human Chondrosarcoma Cells through Reactive Oxygen Species/Mitochondrial Dysfunction and the Caspases Dependent Pathway. Int J Mol Sci. https://doi.org/10.3390/ijms17091491

Lowry OH, Rosebrough NJ, Farr AL, Randall RJ (1951) Protein measurement with the Folin phenol reagent. J Biol Chem 193(1):265–275

Martins MJ, Roque Bravo R, Enea M, Carmo H, Carvalho F, Bastos ML et al (2018) Ethanol addictively enhances the in vitro cardiotoxicity of cocaine through oxidative damage, energetic deregulation, and apoptosis. Arch Toxicol 92(7):2311–2325. https://doi.org/10.1007/s00204-018-2227-7

McDonald MG, Rettie AE (2007) Sequential metabolism and bioactivation of the hepatotoxin benzbromarone: formation of glutathione adducts from a catechol intermediate. Chem Res Toxicol 20(12):1833–1842. https://doi.org/10.1021/tx7001228

McIntyre IM, Gary RD, Trochta A, Stolberg S, Stabley R (2015) Acute 5-(2-aminopropyl)benzofuran (5-APB) intoxication and fatality: a case report with postmortem concentrations. J Anal Toxicol 39(2):156–159. https://doi.org/10.1093/jat/bku131

McMurtry RJ, Mitchell JR (1977) Renal and hepatic necrosis after metabolic activation of 2-substituted furans and thiophenes, including furosemide and cephaloridine. Toxicol Appl Pharmacol 42(2):285–300

Meyer MR, Vollmar C, Schwaninger AE, Wolf E, Maurer HH (2012) New cathinone-derived designer drugs 3-bromomethcathinone and 3-fluoromethcathinone: studies on their metabolism in rat urine and human liver microsomes using GC-MS and LC-high-resolution MS and their detectability in urine. J Mass Spectrom 47(2):253–262. https://doi.org/10.1002/jms.2960

Monks TJ, Jones DC, Bai F, Lau SS (2004) The role of metabolism in 3,4-(+)-methylenedioxyamphetamine and 3,4-(+)-methylenedioxymethamphetamine (ecstasy) toxicity. Ther Drug Monit 26(2):132–136

Montiel-Duarte C, Varela-Rey M, Oses-Prieto JA, Lopez-Zabalza MJ, Beitia G, Cenarruzabeitia E et al (2002) 3,4-Methylenedioxymethamphetamine ("Ecstasy") induces apoptosis of cultured rat liver cells. Biochim Biophys Acta 1588(1):26–32

Nakagawa Y, Suzuki T, Tada Y, Inomata A (2017) Cytotoxic effects of psychotropic benzofuran derivatives, N-methyl-5-(2-aminopropyl)benzofuran and its N-demethylated derivative, on isolated rat hepatocytes. J Appl Toxicol. https://doi.org/10.1002/jat.3351

Navarro-Yepes J, Burns M, Anandhan A, Khalimonchuk O, del Razo LM, Quintanilla-Vega B et al (2014) Oxidative stress, redox

signaling, and autophagy: cell death versus survival. Antioxid Redox Signal 21(1):66–85. https://doi.org/10.1089/ars.2014.5837
Ormerod MG, Sun XM, Brown D, Snowden RT, Cohen GM (1993) Quantification of apoptosis and necrosis by flow cytometry. Acta Oncol 32(4):417–424
Parmar KR, Jhajra S, Singh S (2016) Detection of glutathione conjugates of amiodarone and its reactive diquinone metabolites in rat bile using mass spectrometry tools. Rapid Commun Mass Spectrom 30(10):1242–1248. https://doi.org/10.1002/rcm.7545
Pedersen AJ, Petersen TH, Linnet K (2013) In vitro metabolism and pharmacokinetic studies on methylone. Drug Metab Dispos 41(6):1247–1255. https://doi.org/10.1124/dmd.112.050880
Perry SW, Norman JP, Barbieri J, Brown EB, Gelbard HA (2011) Mitochondrial membrane potential probes and the proton gradient: a practical usage guide. Biotechniques 50(2):98–115. https://doi.org/10.2144/000113610
Pontes H, Santos-Marques MJ, Fernandes E, Duarte JA, Remiao F, Carvalho F et al (2008a) Effect of chronic ethanol exposure on the hepatotoxicity of ecstasy in mice: an ex vivo study. Toxicol In Vitro 22(4):910–920. https://doi.org/10.1016/j.tiv.2008.01.010
Pontes H, Sousa C, Silva R, Fernandes E, Carmo H, Remiao F et al (2008b) Synergistic toxicity of ethanol and MDMA towards primary cultured rat hepatocytes. Toxicology 254(1–2):42–50. https://doi.org/10.1016/j.tox.2008.09.009
Ramesh Varkhede N, Jhajra S, Suresh Ahire D, Singh S (2014) Metabolite identification studies on amiodarone in in vitro (rat liver microsomes, rat and human liver S9 fractions) and in vivo (rat feces, urine, plasma) matrices by using liquid chromatography with high-resolution mass spectrometry and multiple-stage mass spectrometry: characterization of the diquinone metabolite supposedly responsible for the drug's hepatotoxicity. Rapid Commun Mass Spectrom 28(4):311–331. https://doi.org/10.1002/rcm.6787
Ratz Bravo AE, Drewe J, Schlienger RG, Krahenbuhl S, Pargger H, Ummenhofer W (2005) Hepatotoxicity during rapid intravenous loading with amiodarone: description of three cases and review of the literature. Crit Care Med. 33(1):128–134. https://doi.org/10.1097/01.ccm.0000151048.72393.44 **(discussion 245–6)**
Rickli A, Kopf S, Hoener MC, Liechti ME (2015) Pharmacological profile of novel psychoactive benzofurans. Br J Pharmacol 172(13):3412–3425. https://doi.org/10.1111/bph.13128
Roque Bravo R, Carmo H, Carvalho F, Bastos ML, Dias da Silva D, Benzo fury (2019) A new trend in the drug misuse scene. J Appl Toxicol. https://doi.org/10.1002/jat.3774
Schneider JL, Cuervo AM (2014) Liver autophagy: much more than just taking out the trash. Nat Rev Gastroenterol Hepatol 11(3):187–200. https://doi.org/10.1038/nrgastro.2013.211
Seetohul LN, Pounder DJ (2013) Four fatalities involving 5-IT. J Anal Toxicol 37(7):447–451. https://doi.org/10.1093/jat/bkt053
Smith GF (2011) Designing drugs to avoid toxicity. Prog Med Chem 50:1–47. https://doi.org/10.1016/B978-0-12-381290-2.00001-X
Takai S, Oda S, Tsuneyama K, Fukami T, Nakajima M, Yokoi T (2016) Establishment of a mouse model for amiodarone-induced liver injury and analyses of its hepatotoxic mechanism. J Appl Toxicol 36(1):35–47. https://doi.org/10.1002/jat.3141
Tsuda T, Tada H, Tanaka Y, Nishida N, Yoshida T, Sawada T et al (2018) Amiodarone-induced reversible and irreversible hepatotoxicity: two case reports. J Med Case Rep. 12(1):95. https://doi.org/10.1186/s13256-018-1629-8
Turcant A, Deguigne M, Ferec S, Bruneau C, Leborgne I, Lelievre B et al (2017) A 6-year review of new psychoactive substances at the Centre antipoison Grand-Ouest d'Angers: Clinical and biological data. Toxicologie Analytique et Clinique. 29(1):18–33. https://doi.org/10.1016/j.toxac.2016.12.001
UNODC (2018) World Drug Report: United Nations Office on Drugs and Crime 2018 June 2018
Valente MJ, Araujo AM, Bastos ML, Fernandes E, Carvalho F, Guedes de Pinho P et al (2016) Characterization of hepatotoxicity mechanisms triggered by designer cathinone drugs (beta-Keto Amphetamines). Toxicol Sci 153(1):89–102. https://doi.org/10.1093/toxsci/kfw105
Valente MJ, Amaral C, Correia-da-Silva G, Duarte JA, Bastos ML, Carvalho F et al (2017) Methylone and MDPV activate autophagy in human dopaminergic SH-SY5Y cells: a new insight into the context of beta-keto amphetamines-related neurotoxicity. Arch Toxicol 91(11):3663–3676. https://doi.org/10.1007/s00204-017-1984-z
Vallersnes OM, Persett PS, Oiestad EL, Karinen R, Heyerdahl F, Hovda KE (2017) Underestimated impact of novel psychoactive substances: laboratory confirmation of recreational drug toxicity in Oslo, Norway. Clin Toxicol (Phila) 55(7):636–644. https://doi.org/10.1080/15563650.2017.1312002
Verhovez A, Elia F, Riva A, Ferrari G, Apra F (2011) Acute liver injury after intravenous amiodarone: a case report. Am J Emerg Med 29(7):843.e5-6. https://doi.org/10.1016/j.ajem.2010.03.035
Waldhauser KM, Torok M, Ha HR, Thomet U, Konrad D, Brecht K et al (2006) Hepatocellular toxicity and pharmacological effect of amiodarone and amiodarone derivatives. J Pharmacol Exp Ther 319(3):1413–1423. https://doi.org/10.1124/jpet.106.108993
Welter J, Brandt SD, Kavanagh P, Meyer MR, Maurer HH (2015a) Metabolic fate, mass spectral fragmentation, detectability, and differentiation in urine of the benzofuran designer drugs 6-APB and 6-MAPB in comparison to their 5-isomers using GC-MS and LC-(HR)-MS(n) techniques. Anal Bioanal Chem 407(12):3457–3470. https://doi.org/10.1007/s00216-015-8552-2
Welter J, Kavanagh P, Meyer MR, Maurer HH (2015b) Benzofuran analogues of amphetamine and methamphetamine: studies on the metabolism and toxicological analysis of 5-APB and 5-MAPB in urine and plasma using GC-MS and LC-(HR)-MS(n) techniques. Anal Bioanal Chem 407(5):1371–1388. https://doi.org/10.1007/s00216-014-8360-0
Wu Q, Ning B, Xuan J, Ren Z, Guo L, Bryant MS (2016) The role of CYP 3A4 and 1A1 in amiodarone-induced hepatocellular toxicity. Toxicol Lett 253:55–62. https://doi.org/10.1016/j.toxlet.2016.04.016
Yuan L, Kaplowitz N (2013) Mechanisms of drug-induced liver injury. Clin Liver Dis 17(4):507–518. https://doi.org/10.1016/j.cld.2013.07.002
Zhang Y, Chen X, Gueydan C, Han J (2018) Plasma membrane changes during programmed cell deaths. Cell Res 28(1):9–21. https://doi.org/10.1038/cr.2017.133